DISSERTATIONES MEDICINAE UNIVERSITATIS TARTUENSIS
177

DISSERTATIONES MEDICINAE UNIVERSITATIS TARTUENSIS
177

MALLE KUUM

Mitochondrial and endoplasmic reticulum cation fluxes: Novel roles in cellular physiology

TARTU UNIVERSITY
PRESS

Department of Pharmacology, Centre of Excellence for Translational Medicine, University of Tartu, Ravila 19, 50411 Tartu, Estonia

Dissertation is accepted for the commencement for the degree of Doctor of Medical Sciences on September 22, 2010 by the Council of the Faculty of Medicine, University of Tartu, Estonia

Supervisors: Allen Kaasik, PhD, Professor, Department of Pharmacology, University of Tartu.

Vladimir Veksler, MD, PhD, Professor, INSERM U-769, Faculté de Pharmacie, Université Paris-Sud, Châtenay-Malabry, France

Reviewers: Enn Seppet, MD, PhD, Professor, Department of General and Molecular Pathology, University of Tartu

Marko Vendelin, PhD, Wellcome Trust International Senior Research Fellow, Institute of Cybernetics, Tallinn University of Technology

Opponent: Gyorgy Szabadkai, MD, PhD, Senior Lecturer, PI, Department of Physiology, currently Department of Cell and Development, Faculty of Life Sciences, University College London, UK

Commencement: November 22, 2010

This Research was supported by the European Regional Development Fund and by the European Union through the European Social Fund.

Publication of this dissertation is granted by the University of Tartu

ISSN 1024–395X
ISBN 978–9949–19–494–0 (trükis)
ISBN 978–9949–19–495–7 (PDF)

Tartu Ülikooli Kirjastus
www.tyk.ee
Tellimus nr 582

To my family

TABLE OF CONTENTS

3

LIST OF ORIGINAL PUBLICATIONS

1. Kaasik A, Safiulina D, Choubey V, **Kuum M**, Zharkovsky A, Veksler V. (2007) Mitochondrial swelling impairs the transport of organelles in cerebellar granule neurons. *The Journal of Biological Chemistry.* 282(45); 32821–32826.

2. **Kuum M**, Kaasik A, Joubert F, Ventura-Clapier R, Veksler V. (2009) Energetic state is a strong regulator of sarcoplasmic reticulum Ca^{2+} loss in cardiac muscle: different efficiences of different energy sources. *Cardiovascular Research.* 83(1):89–96.

3. Kaasik A, **Kuum M,** Joubert F, Wilding J, Ventura-Clapier V, Veksler V. (2010) Mitochondria as a source of mechanical signals in cardiomyocytes. *Cardiovascular Research.* 87(1):83–91.

4. **Kuum M,** Veksler V, Liiv J, Ventura-Clapier R, Kaasik A. Potassium-hydrogen exchanger and small conductance calcium-activated potassium channel are essential for endoplasmic reticulum calcium uptake. (Manuscript).

Contribution of the author:

1. The author analysed part of the organelle movement experiments and assisted in writing the manuscript.

2. The author performed all of the experiments except imaging, analysed the results and participated in writing the manuscript.

3. The author did all of the experiments with the cardiac fibres, analysed the data and participated in writing the manuscript.

4. The author performed all of the experiments with the cardiac fibres, immunochemistry, Western blot analysis, part of the flusorescence experiments, analysed the results and participated in writing the manuscript.

ABBREVATIONS

$[Ca^{2+}]$	Ca^{2+} concentration
5-HD	sodium 5-hydroxydecanoate
BES	*N*, *N*-bis(2-hydroxyethyl)-2-aminoethanesulfonic acid
BK_{Ca}	large-conductance Ca^{2+} dependent K^+ channel
CK	creatine kinase
CPA	cyclopiazonic acid
EGTA	ethylene glycol-bis(β-aminoethyl ether)*N*, *N*, *N*′,*N*′-tetra-acetic acid
ER	endoplasmic reticulum
IK_{Ca}	intermediate-conductance Ca^{2+} dependent K^+ channel
IP_3R	inositol 1,4,5- triphosphate receptors
K_{ATP}	ATP dependent K^+ channel
K_{Ca}	Ca^{2+} dependent K^+ channel
KHE	K^+–H^+ exchanger
MAM	mitochondria-associated ER-membrane
NHE	Na^+–H^+ exchanger
PCr	phosphocreatine
Pi	inorganic phosphate
PTP	permeability transition pore
RyR	ryanodine receptors
SERCA	SR/ER Ca^{2+}-dependent ATPase
SK_{Ca}	small conductance Ca^{2+} dependent K^+ channel
SR	sarcoplasmic reticulum
SR/ER	sarcoplasmic/endoplasmic reticulum
TBQ	2,5-di(tert-butyl)hydroquinone
TEA^+	tetraethylammonium ion
TG	thapsigargin
WHS	Wolf-Hirschhorn Syndrome

INTRODUCTION

Cationic fluxes across intracellular membranes play essential roles in the functioning of membranous organelles like mitochondria and the sarcoplasmic/ endoplasmic reticulum (SR/ER). It is generally accepted that intracellular transmembrane cationic fluxes are indispensable for ATP production, mitochondrial dynamics, cell excitability and/or contraction, redox homeostasis and many other processes. Cation (particularly Ca^{2+}) fluxes across the SR/ER membrane determine many essential processes in excitable cells such as cardiomyocytes and neurons. Some fluxes driven by ATPases (for example, Ca^{2+} ATPase) against a concentration gradient need a strong energy support to maintain a high ATP/ADP ratio near the pumps.

Mitochondria are known as the mobile power plants of the cell because of their ability to generate ATP and to change spatial organization depending on local energy demand. In addition to ATP synthesis, mitochondria are the site of other important metabolic reactions, including steroid hormone and porphyrin synthesis, the urea cycle, lipid metabolism, and the interconversion of amino acids (Brookes *et al.*, 2004). Although the mitochondrion is a separated organelle, its function and functioning within the cell is tightly connected to SR/ER functioning and vice versa. Together they control different aspects of cellular metabolism and there is a tight functional coupling between them which involves Ca^{2+} handling, signalling pathways including activation of cell death mechanisms, and enzyme synthesis, amongst others.

It has been shown by several studies that changes in mitochondrial ion homeostasis and membrane potential may lead to changes in the basic functions of mitochondria and also to changes in its volume and geometry (Halestrap, 1989; Juhazova *et al.*, 2004; Kaasik *et al.*, 2007; Safiulina *et al.*, 2006). These changes are especially important in cells where organelles are highly organized, like in mammalian cardiomyocytes (Dhalla *et al.*, 2009; Vendelin *et al.*, 2004 and references therein), or where they match the size of intracellular spaces, as in neurons (Benquet *et al.*, 2002; Kaasik *et al.*, 2007; Safiulina *et al.*, 2006; Shepherd and Harris, 1998). These changes have been associated with a wide range of important biological functions and pathologies. For example, defects in axonal transport are indirectly linked to several progressive human neurodegenerative diseases including Alzheimer's disease, Huntington's disease and amyotrophic lateral sclerosis. Swollen mitochondria are able to mediate mechanical signals that affect their neighbouring structures in cardiomyocytes by increasing the contractility in ATP and Ca^{2+} in an independent manner (Kaasik *et al.*, 2004). It has been suggested that mitochondrial volume modifications could also have an important impact also on other mitochondria-rich cell types such as neurons (Kaasik *et al.*, 2007). However, the role of ion flux-induced changes in mitochondrial geometry has not been investigated.

In the cell, maintenance of Ca^{2+} homeostasis is an ATP-dependent process so that alterations in mitochondrial energy producing or in energy transport

systems may lead to imbalanced Ca^{2+} handling. Changes in Ca^{2+} concentration in the SR/ER lumen and cytosol may lead to a dysfunction of the cell or even to the activation of cell death mechanisms by causing mitochondrial Ca^{2+} overload. Importantly, the intra/extrareticular balance of Ca^{2+} depends not only on SR/ER Ca^{2+} uptake but also on transmembrane Ca^{2+} leak during period of rest. This leak is suggested to be a Ca^{2+} efflux through calcium-sensitive calcium release channels, ryanodine receptors, or through the reversal of SR/ER ATP-dependent Ca^{2+} pumps (SERCA). It has been suggested that Ca^{2+} loss through Ca^{2+} pumps is sensitive to the cellular energetic state (Shannon *et al*., 2002). An increased Ca^{2+} leak may lead to cell pathologies or to be an additional factor in the development of heart failure. Such an important question needs to be studied.

Theoretically, Ca^{2+} fluxes in the SR/ER are able to induce a significant redistribution of the electrochemical potential across the SR/ER membrane. However, despite the ongoing movement of Ca^{2+} ions, the SR/ER membrane maintains its electroneutrality. This means that Ca^{2+} uptake and release must be equilibrated by fluxes of some counter-ions such as K^+, Na^+ or Cl^-. The dependence of Ca^{2+} fluxes in the SR/ER membrane on K^+ concentration in the cytosol and in the SR/ER has been known for decades (Abramcheck and Best, 1989; Liu and Strauss, 1991). It is also known that Ca^{2+} uptake by SERCA is coupled to H^+ efflux (Levy, 1990 and references therein) and some mechanisms must exist to prevent high pH shifts in the vicinity of SERCA. However, ion fluxes through the SR/ER membrane, which could compensate for Ca^{2+} and H^+ fluxes across the SR/ER membrane, are poorly studied.

Accordingly, in the present study, we investigated how the swelling of mitochondria, which is controlled by transmembrane cationic fluxes, may change the functional properties of two types of excitable cells: neurons and cardiomyocytes. We studied the effects of mitochondrial swelling on organelle trafficking in neurite shafts and on properties of myofibrillar and nuclear compartments. Furthermore, we investigated the regulation of transmembrane Ca^{2+} fluxes in the SR/ER. Firstly, we studied the control of transmembrane Ca^{2+} fluxes by SR/ER potassium homeostasis. Secondly, we studied the pathways of passive Ca^{2+} efflux from cardiomyocytes, and their dependence on the energetic state of the cell.

BACKGROUND OF THE STUDY

1. Mitochondria

1.1. Mitochondrial structure

The mitochondrion is a membrane-enclosed organelle found in most eukaryotic cells. A mitochondrion contains outer and inner membranes composed of phospholipid bilayers and proteins. The outer mitochondrial membrane is permeable to most ions and nutrients with a molecular mass of up to 5000 daltons passing through the membrane through the porin channel. Larger molecules and proteins can only traverse the outer membrane by using specific carriers or protein import machinery. The inner membrane is highly convoluted and forms internal compartments known as cristae. The highly folded inner membrane greatly increases the total surface area and houses the electron transport chain together with ATP synthetase as well as transport proteins for ions and metabolites. The space inside the inner membrane is called the mitochondrial matrix and it contains soluble enzymes which catalyse the oxidation of pyruvate and fatty acids, mitochondrial ribosomes and mitochondrial DNA (Alberts *et al*., 2002).

1.2. Mitochondrial function

The main function of mitochondria is to produce ATP by oxidative phosphorylation. In the mitochondrial matrix, acetyl coenzyme A (a product of pyruvate or fatty acid oxidation) enters the Krebs cycle giving the reduced equivalents (NADH and $FADH_2$). These equivalents are oxidized in a series of reactions catalysed by the electron transport chain in the mitochondrial inner membrane, where electrons finally pass to oxygen, which is reduced to water. The chemical energy liberated in these reactions is used to export protons from the matrix into the intermembrane space, thus creating an electrochemical proton gradient (–150 to –200 mV) across the inner mitochondrial membrane. This gradient then is used as a driving force for ATP synthetase to produce ATP from ADP and inorganic phosphate.

Mitochondria also act as an intracellular Ca^{2+} store. Their strategic localization close to the spots of intracellular Ca^{2+} release makes them very good "cytosolic buffers" for Ca^{2+} (Duchen, 2000). They are also key players in cell death mechanisms. Opening of the membrane permeability transition pore (PTP), a nonselective, high conductance channel, leads to the release of cytochrome c and other apoptotic factors, triggering the activation of caspase cascades. Besides these, mitochondria participate in many other cellular processes which are out of the scope of this study.

1.3. Mitochondrial dynamics

Mitochondria need to be in close spatial localization with other cell organelles for the most efficient use of the energy they produce. In densely packed and mitochondria rich cell types like in cardiomyocytes, the mitochondria are localized close to the energy consuming structures and direct energetic cross-talk between mitochondria and the ATPases of the sarcoplasmic reticulum has been demonstrated (Kaasik *et al.*, 2001).

In contrast to cardiomyocytes where mitochondria are stationary organelles, the neuronal mitochondria are highly motile. With the help of motor proteins – kinesins, dyneins and myosins, the mitochondria are transported along cytoskeletal tracks to areas where the energy demands are high and/or where calcium buffering is required (Duchen, 2000; Gunter *et al.*, 2000; Hollenbeck and Saxton, 2005; Reis *et al.*, 2009). Such mitochondrial trafficking is particularly important for neurons, where mitochondria are obliged to travel considerable distances along axons to supply synaptic endings with the energy needed for neurotransmitter release and recycling (Chen and Chan, 2006). It should be noted here that mitochondria must be transported through the slender, highly branched neuronal processes: the axonal shafts between the varicosities are extremely thin, with mean diameter of around 200–300 nm (Benquet *et al.*, 2002; Shepherd and Harris, 1998) that matches the diameter of mitochondria (Kaasik *et al.*, 2007; Safiulina *et al.*, 2006). It has been shown that even small perturbations of mitochondrial dynamics can, over time, give rise to severe effects in neurons. Aberrant mitochondrial dynamics can contribute to the pathogenesis of late-onset neurodegenerative conditions such as amyotrophic lateral sclerosis, Huntington's, Parkinson's and Alzheimer's diseases (Shi *et al.*, 2010; Su *et al.*, 2010 and references therein; Wang *et al.*, 2009).

1.4. Mitochondrial volume homeostasis

Mitochondrial volume homeostasis is a housekeeping function essential for maintaining the structural integrity of the organelle. Changes of mitochondrial volume may strongly modulate mitochondrial physiology and be a key issue in cellular pathophysiology. There are two principally different ways of controlling mitochondrial size. Mitochondria frequently fuse and divide, and the balance of these processes determines overall mitochondrial morphology. Another possibility is related to water movement into and out of mitochondria. The inner mitochondrial membrane is impermeable to most ions and their flux and concentrations in the mitochondrial matrix are controlled by specific channels and exchangers, whereas water flux into and out of mitochondria is mainly determined by the osmotic gradient between the cytosol and the matrix. Osmotic balance between the cytosol and the matrix determines water movement (whether it passes through the inner membrane by simple diffusion

through the lipid bilayer or accompanies ions through the channels or through specific water channels: aquaporins) between these two compartments, by which the mitochondrial matrix volume is influenced.

It has been suggested that the abovementioned osmotic balance in mitochondria is mainly controlled by mitochondrial potassium fluxes. Moreover, it has been suggested that altered potassium fluxes could also mediate the mitochondrial matrix volume changes observed with depolarization, Ca^{2+} overload and opening of the PTP (Kaasik *et al.*, 2007).

2. Endoplasmic reticulum

2.1. Structure and distribution of the endoplasmic reticulum

The endoplasmic reticulum (ER) is the largest single intracellular organelle which appears as a three-dimensional network formed by an endomembrane. Its structural organization is extremely variable, being organized in a complex system of microtubules and cisternae; this organization depends on its functions. The most obvious structural heterogeneity concerns the division of the ER into two different forms: rough ER with associated ribosomes which is involved in protein synthesis, correct post-translational "folding" of these proteins and Ca^{2+} signalling; and smooth ER which is mainly responsible for Ca^{2+} signalling; and the nuclear membrane. In muscle cells, the ER is arranged in series of ranks with the sarcomers and is called the sarcoplasmic reticulum (SR), which ensures the synchronous release of Ca^{2+} and the creation of the rapid global signals necessary to contract the large muscle cells. In neurons, the ER extends from the nuclear envelope to axons and presynaptic terminals, as well as to dendrites and dendritic spines which are much less organized.

2.2. Function of endoplasmic reticulum

The ER is a multifunctional signalling organelle regulating a wide range of cellular processes. One of its primary functions is the regulation of cytosolic Ca^{2+} concentration. The ER is a source of the Ca^{2+} ions that are released through either inositol 1,4,5-trisphosphate – sensitive receptors (IP_3R) or ryanodine – sensitive receptors (RyR), and it removes Ca^{2+} from the cytosol by the SERCA.

The ER also serves as a common transport route through which numerous proteins are delivered to their destination (Palade, 1975). The ER also plays a central role in sterol biosynthesis, on the one hand through sensing the level of sterols by having sterol regulatory element-binding proteins in its membrane, and on the other by providing output signals that make the necessary adjustments to lipid synthesis to maintain a constant level of membrane cholesterol. The ER takes part in the modulation of inflammatory reactions and

the regulation of signalling enzymes by being one of the membranes to which cytosolic phospholipase A2, the enzyme that hydrolyses lipid precursors in the ER to release arachidonic acid, is associated. Another important function of the ER is in taking part in activating cell death mechanisms by activating apoptosis upon the release of caspase-12 from the ER membrane by proteolytic cleavage following ER stress or by involving the ER/mitochondrial couple (Berridge, 2002).

3. Physiological role of interactions between the ER, mitochondria and other cellular organelles

3.1. Mitochondria-associated membranes and calcium crosstalk

The mitochondrial outer membrane can associate with the ER membrane, in a structure called the mitochondria-associated ER-membrane (MAM). Such contacts are crucial for the synthesis and intracellular transport of phospholipids, as well as for intracellular Ca^{2+} signalling and for the determination of mitochondrial structure (for a review, see Lebiedzinska *et al*., 2009). In the MAM area, distances between mitochondrial and the ER membrane are very short and membranes are adjoined by tethers that are ~10 nm at the smooth ER and ~25 nm at the rough ER (Csordas *et al.*, 2006). The possible occurrence of functional microcompartments created by juxtaposed contact sites between mitochondria and the ER sufficient for the synthesis and transfer of phospholipids derived from serine has been suggested by different authors (Ardail, 1993; Vance, 1990). It is proposed that MAMs which participate in intracellular calcium signalling are formed in the SR/ER membrane facing mitochondria, where channels releasing Ca^{2+} (IP_3R and RyR) are concentrated into clusters and form functional units that communicate with juxtaposed mitochondrial Ca^{2+} uptake sites (Hajnoczky *et al*., 2000; Lebiedzinska *et al.*, 2009 and references therein).

It is also known that mitochondrial Ca^{2+} homeostasis synchronizes ATP generation with the energy needs of the cell. Increased Ca^{2+} concentrations ($[Ca^{2+}]$) in the cytoplasm will increase matrix Ca^{2+} level which in turn will stimulates dehydrogenases of the Krebs cycle and enhances the electron flow through the electron transport chain and increasing ATP production (Brookes *et al.*, 2004; Cortassa *et al*., 2003; Jouaville *et al*., 1999). Such cooperation between mitochondria and the SR has been best demonstrated in the heart where increase in cardiac workload increased the cytoplasmic $[Ca^{2+}]$ and increased the mitochondrial ATP production (Harris and Das, 1991; Territo *et al.*, 2000, 2001).

3.2. Energetic crosstalks between the mitochondria and the SR/ER

Recent reports suggest the existence of energetic communication between mitochondria and the SR/ER. The Ca^{2+} uptake of SR/ER requires a constant ATP supply to create a high ATP/ADP ratio near the SERCA. ATP can reach for these energy demanding areas by passive diffusion, by facilitated diffusion or by direct channelling from closely located mitochondria or glycolytic machinery (Boehm *et al*., 2000; Kaasik *et al*., 2001). It has been shown that in cardiomyocytes, where the SR/ER energy need is the highest, the Ca^{2+} uptake by SERCA can be efficiently supported by direct energy channelling from mitochondria and by creatine kinase mediated energy channelling (Kaasik *et al*., 2001). Consistent with this direct ATP channelling theory, Saks *et al*. (2001) demonstrated that mitochondria can directly withdraw ADP from myofibrils/SR. Furthermore, it has been shown that in cardiac muscle, cytoarchitecture disturbances lead to alterations in the direct transfer of energy from mitochondria to SERCA (Wilding *et al*., 2006).

4. Intracellular potassium channels and exchangers

4.1. Classification of the intracellular potassium channels and exchangers

There are four major classes of potassium channels in the cell mostly located in the plasma membrane: inwardly rectifying potassium channels, calcium-activated potassium channels, tandem pore domain potassium channels and voltage-gated potassium channels. From inwardly rectifying potassium channels, only a subclass of ATP-dependent channels (K_{ATP}) was shown to also have an intracellular localization. Mitochondrial localization of K_{ATP} channels was thoroughly reviewed by Bernardi (1999) and Garlid and Paucek (2003), and more recently Zhou *et al*. (2005) demonstrated that, K_{ATP} channels are also present in other intracellular sites, including the ER. A number of pharmacological openers (diazoxide, cromacalim) as well as inhibitors (glibenclamide, sodium 5-hydroxydecanoate (5-HD)), are known to modulate these channels. However, they have no specificity towards the intracellular channels and affect plasma membrane K_{ATP} channels as well.

From the calcium-activated potassium channels (K_{Ca}), the large-conductance Ca^{2+}-dependent K^+ channel (BK_{Ca}) has been shown to also be located in mitochondria (Nowikovsky *et al*., 2009 and references therein) and the ER membrane (Yamashita *et al*., 2006). These BK_{Ca} channels can be opened by NS 1619 (Bednarczyk, 2009 and references therein) and blocked by scorpion-venom toxins charybdotoxin, iberiotoxin and paxilline (Szewczyk *et al*., 2006).

Similarly to K_{ATP} channel modulators, these compounds also affect plasma membrane BK_{Ca} channels. No intracellular localization of the other K_{Ca} channels, the small conductance (SK_{Ca}) and intermediate conductance (IK_{Ca}) calcium-dependent potassium channels has been demonstrated to date.

Potassium flux across intracellular membranes could also be controlled by the K^+–H^+ exchanger (KHE). Its localization in the inner mitochondrial membrane is well established although its molecular nature has remained under question. The KHE is known to be regulated by Mg^{2+} and H^+ in the matrix, the matrix volume and quinine, and irreversibly inhibited by dicyclohexylcarbodiimide (DCCD) (Bernardi, 1999). The *MDM38/YOL027cp* gene has been identified as an essential gene for mitochondrial KHE activity and for respiratory growth in yeast cells. Strong evidence for the role of this gene in KHE expression came from the finding that nigericin, a substance which is known to ensure electroneutral K^+/H^+ exchange, restored aerobic growth in Mdm38p/Yol027cp-null yeast strains and reverted mitochondrial swelling *in situ*. The human homologue for this gene is known as *LETM1*. It is not clear whether these proteins constitute the KHE itself or whether they are an essential component allowing the exchange activity to take place (Nowikovsky *et al*., 2004, 2007, 2009).

4.2. Relevance of intracellular potassium fluxes in mitochondria

It has been suggested that the main role of mitochondrial K^+ channels, as well as mitochondrial K^+ fluxes, in general, is to govern mitochondrial volume homeostasis. Mitochondrial volume homeostasis is a housekeeping function essential for maintaining the structural integrity of the organelle. Changes in mitochondrial volume may strongly modulate mitochondrial physiology and be a key issue in cellular pathophysiology. Recently, it was suggested that mitochondrial swelling could have other effects on cell function. The results obtained by Kaasik *et al*. (2004) suggest that, in cardiomyocytes, an increase in mitochondrial volume can impose mechanical constraints inside the cell. However, the possible consequences of such an intracellular mechanical impact have not yet been investigated.

Such a mechanical signalling could also exist in neurons. Mitochondrial traffic in axonal shafts could be very sensitive to mitochondrial volume modulations because the diameter of these shafts precisely matches mitochondrial diameter under normal conditions (Benquet *et al*., 2002; Kaasik *et al*., 2007; Safiulina *et al*., 2006; Shepherd and Harris, 1998). Therefore, a temporal increase in mitochondrial size (induced either by a cation influx or disruption of mitochondrial potential) could be one of the factors regulating mitochondrial traffic in neurites.

In living cells, alterations in mitochondrial potassium flux control may be related to Wolf-Hirschhorn Syndrome (WHS) which is a complex disease involving the central nervous system and is caused by the partial, heterozygous deletion of the terminal portion of the short arm of one chromosome 4 involving the 4p16.3 region (Nowikovsky *et al*., 2009). It causes severe growth and mental retardation, hypotension, midline fusion defects and typical facial dysmorphism seizures and poor muscle tone, amongst others (Johnson *et al*., 1976; Wilson *et al*., 1981; Zollino, 2000). According to genetic studies on WHS patients, deletion of the human KHE gene *LETM1* (and therefore, alteration in the KHE) is likely to be responsible for the development of this disease (Nowikovsky *et al*., 2009).

4.3. Relevance of potassium fluxes in the endoplasmic reticulum

Efficient Ca^{2+} uptake coupled to electrical charge displacement should be accompanied by counter-ion movements across the ER. A lack of such counter flux would develop a membrane potential which would oppose further Ca^{2+} pumping to the ER. Indeed, translocation of Ca^{2+} ions to the ER lumen by SERCA is associated by the counter transport of protons to ensure partial charge balancing (Levy *et al.*, 1990). However, the basal level of protons in the lumen is only around 10^{-7}M and could not compensate for a relatively massive calcium ion entry into the reticulum; moreover, such a proton flux could induce a considerable pH change in the lumen and compromise the SERCA function (Peinelt and Apell, 2002). Therefore, it is reasonable to suggest that Ca^{2+} flux across the SR/ER membrane is coupled to counter fluxes of intracellular ions (first of all, K^+), which could equilibrate the transmembrane potential. However, there is still no clear-cut evidence demonstrating whether or not K^+ fluxes are important for ER Ca^{2+} uptake. Moreover, it is also not clear which types of K^+ channels are present in the SR/ER membrane.

5. Intracellular calcium fluxes

5.1. Intracellular calcium pumps and channels

Compared with potassium handling pathways which seem rather similar for the ER and mitochondria, the Ca^{2+} handling of these structures is rather different. Entry of Ca^{2+} into the mitochondrial matrix is controlled by the mitochondrial Ca^{2+} uniporter, whereas its extrusion from the matrix occurs through the Na^+-Ca^{2+} exchanger. The Ca^{2+} uniporter is regulated by divalent cations and adenine nucleotides, and inhibited by ruthenium red (Bernardi, 1999; Colegrove *et al*., 2000). In addition, two previously unknown Ca^{2+}-selective voltage-

dependent channels referred to as mCa1 and mCa2 were identified by patch clamping the inner membrane of mitochondria from human hearts (Michels *et al*., 2009). Calcium is primarily extruded from the matrix through the Na^+-Ca^{2+} exchanger in exchange for Na^+, and Na^+ is further exchanged for protons by the Na^+-H^+ exchanger (NHE) (Bernardi, 1999; Dash and Beard, 2008; Gunter and Pfeiffer, 1990). Another Ca^{2+} efflux pathway is the Na^+-independent Ca^{2+}-exchange pathway for Ca^{2+} extrusion from the matrix, possibly by the Ca^{2+}-H^+ exchanger found in some tissues such as the liver (Gunter and Pfeiffer, 1990).

In contrast to the mitochondria, Ca^{2+} uptake into SR/ER is driven by ATP-dependent Ca^{2+} pumps. These include three gene products SERCA1, SERCA2 and SERCA3 (alternative splicing produces two distinct isoforms of SERCA2, namely, 2a and 2b). The SERCA1 is exclusively expressed in fast skeletal muscle, SERCA2 is ubiquitously expressed, and SERCA3 is considered to be mainly expressed in cells of the haematopoietic lineage and in some epithelial cells (for a review, see Verkhratsky, 2005 and references therein). SERCA utilizes the free energy of ATP to transport Ca^{2+} against the concentration gradient and it has been shown that Ca^{2+} uptake is strongly dependent on energetic conditions in the vicinity of the SERCA pump (Kaasik *et al*., 2001). It can be irreversibly be blocked by thapsigargin (TG) and reversibly blocked by 2,5-di(tert-butyl)hydroquinone (TBQ) and cyclopiazonic acid (CPA). The rate of Ca^{2+} pumping is controlled by the Ca^{2+} concentrations in the ER lumen and in the cytoplasm. Another factor which has been suggested as regulating Ca^{2+} uptake, and which is very poorly studied, is the movement of counter-ions.

The Ca^{2+} efflux from the SR/ER is executed by two families of Ca^{2+} channels, the Ca^{2+}-gated Ca^{2+} channels, generally referred to as RyR, and the inositol 1,4,5-triphosphate (IP_3) – gated channels, commonly known as IP_3R. Functional activity of IP_3Rs is controlled by both IP_3 and cytosolic free Ca^{2+}, whereas RyRs are directly activated by cytosolic [Ca^{2+}]. In neurons, both RyR and IP_3R types of Ca^{2+}-release channels are expressed whereas cardiomyocytes express a significantly larger number of RyRs compared to IP_3Rs. The RyR is considered to be the major pathway for Ca^{2+} efflux, which is important for muscle contraction. On the other hand, IP_3R may play crucial roles in subsarcolemmal, bulk cytoplasmic and nuclear Ca^{2+} signalling in cardiomyocytes (Kockskämper *et al*., 2008).

5.2. Relevance of Ca^{2+} fluxes in mitochondria and SR/ER

Both organelles act as intracellular Ca^{2+} stores. Whilst the role of the SR/ER as intracellular Ca^{2+} storage has been well established for decades, the role of mitochondria in Ca^{2+} homeostasis has remained less studied for a long time. However, it is now widely accepted that mitochondria can act as a sponge to buffer Ca^{2+} despite a low global cytosolic Ca^{2+} concentration and the low

affinity of the mitochondrial Ca^{2+} uniporter (Gustafsson and Gottlieb, 2008; Werth and Thayer, 1994). Mitochondrial signals are relatively rapid and transient because of their position near the cytosolic mouth of the Ca^{2+} channels localized in either the opposing SR/ER or in the plasma membrane (Rizzuto, 1998) where they can capture a substantial amount of the released Ca^{2+}. This ability helps to prevent the level of Ca^{2+} in the cytosol from becoming too high and to avoid SR/ER depletion by recycling Ca^{2+} to the SR/ER (Arnaudeau *et al*., 2001).

Next to the regulation of energy metabolism by mitochondrial matrix [Ca^{2+}] changes as described earlier, mitochondrial Ca^{2+} fluxes are able to induce mitochondrial matrix Ca^{2+} overload, which could be associated with cell injury and the activation of mechanisms of apoptosis. Therefore, during last decades, modulations of matrix volume by Ca^{2+} fluxes were actively discussed as a new topic of interest.

In neuronal cells, the level and dynamic changes in free Ca^{2+} concentration within the ER lumen determine the function of the ER as a Ca^{2+} signalling organelle, and regulate the activity of resident intra-ER enzymatic cascades. Consequently, the cell is vulnerable to disturbances in Ca^{2+} handling by the ER. Severe and persistent disturbances of Ca^{2+} handling by the ER may become a source of cell death signals. This is particularly important for numerous pathological processes in which the disruption of ER Ca^{2+} homeostasis may be implicated as a triggering factor for many forms of cellular pathology (for a review, see Verkhratsky and Toescu, 2003). Changes in ER Ca^{2+} handling and cellular Ca^{2+} homeostasis are important in the development of several neuro-degenerative diseases such as Alzheimer's disease, Huntington's disease and different gangliosidoses. They may also account for cell damage in brain ischaemia and excitotoxicity and be involved in the pathogenesis of diabetic neuropathies (Verkhratsky, 2005).

In the heart, the SR is the central element in excitation-contraction coupling (coupling between electrical excitation of the myocyte and cell contraction). Calcium is an essential ion for cardiac electrical activity and it is also the direct activator of the myofilaments which cause contraction. (Bers, 2003). Contraction of cardiomyocytes depends on the amount of Ca^{2+} released from the SR lumen. It is also generally agreed, that in many cases, compromised contraction is due to reduced SR Ca^{2+} release or weakened SR Ca^{2+} uptake. Therefore, myocyte mishandling of Ca^{2+} is a central cause of both contractile dysfunction and arrhythmias under pathophysiological conditions (Hasenfuss *et al*., 2002). Alterations in transsarcolemmal Ca^{2+} current and action potential characteristics are also seen in heart failure, but the central factor limiting Ca^{2+} transient amplitude is a decrease in SR Ca^{2+} content (Bers, 2003 and references therein).

5.3. Calcium leak

Diminished SR Ca^{2+} content may arise not only from reduced Ca^{2+} uptake but also from increased SR Ca^{2+} loss. In contrast to Ca^{2+} uptake and release, which have been largely investigated, Ca^{2+} leakage from the SR in resting conditions is poorly studied. Loss of Ca^{2+} from the ER diminishes the amount of releasable Ca^{2+} and could affect functioning of the cell. There are two main pathways suggested as being responsible for such a leak: leakage via RyR or reverse efflux via SERCA (see Shannon *et al*., 2002; Sobie *et al*., 2006 and references therein). It has been suggested that Ca^{2+} loss through the SERCA is sensitive to cellular energetic state (Shannon *et al*., 2002). This raises the possibility that compromised energetics might favour diastolic SR Ca^{2+} efflux, thus decreasing the amount of releasable Ca^{2+} and thereby altering cardiac contractility. Nevertheless, it is unclear whether or not a SR Ca^{2+} leak through the SERCA exists in the heart, and if so, then whether or not it is sensitive to energetic conditions.

AIMS OF THE STUDY

The general aim was to study morphological and functional interactions (which are controlled by cationic fluxes) of the mitochondria with other organelles.

The specific aims of the study were as follows:

1) To assess whether or not the modulation of mitochondrial volume by altered cationic fluxes affects organelle transport in neurite shafts of cerebellar granular neurons and to study whether or not these changes in organelle transport are related to mitochondrial ATP-generating activity.

2) To study whether or not the modulation of mitochondrial volume by altered cationic fluxes in cardiomyocytes *in situ* is able to have a mechanical impact on the neighbouring compartments (myofibrillar and nuclear ones).

3) To study whether or not potassium fluxes across the SR/ER membrane affect the functional properties of the SR/ER in excitable cells.

4) To investigate what is the main pathway of Ca^{2+} leak from SR in cardiomyocytes and whether or not this leak is sensitive to energetic interactions between mitochondria and the SR.

MATERIALS AND METHODS

1. Preparation of cardiac fibres and mechanical experiments

Three- to six-month-old male C57BL/6 mice were anaesthetized by intra-peritoneal injections of sodium thiopental according to the recommendations of the institutional Animal Care Committee (INSERM, Paris, France). Hearts were removed and rinsed in ice-cold Ca^{2+}-free Krebs solution equilibrated with 95% O_2/5% CO_2. Fibres (diameter 150 to 300 µm) were dissected from the left ventricular papillary muscles. Specific permeabilization of the sarcolemma was achieced by incubating the fibres for 30 min in *basic solution* (described below, in section 1.2 of Materials and methods) containing additionally 50 µg/ml saponin at 4 °C. After permeabilization the fibres were kept in *basic solution* at 4 °C until further use. The permeabilized fibres were tied at both ends with a natural silk thread and mounted on a stainless-steel hook and a force transducer (AE 801, Aker.s Microelectronics, Horton, Norway). The fibres were immersed in 2.5 ml chambers arranged around a disc and placed into a temperature-controlled bath and positioned on a magnetic stirrer in a 22 °C water bath with a magnetic stirrer.

1.1. Passive force measurement

To estimate intracellular compression induced by swollen mitochondria, we measured the passive force developed by saponin-permeabilized fibres. The passive characteristics (passive force, stiffness) of cardiac myofilaments are known to be very sensitive to mechanical compression associated with a decrease in lattice spacing (Martyn *et al*., 2004; Roos and Brady, 1990). To measure the changes in passive force changes, at the beginning of each experiment the fibre was adjusted to the slack length (sarcomere length 1.85–1.9µm) in *basic solution for measuring passive force* containing (in mM): N,N-bis[2-hydroxyethyl]-2-aminoethanesulfonic acid 60 (BES, pH 7.1), free Mg^{2+} 1, MgATP 3.16, phosphocreatine (PCr) 12, K_2HPO4 3, and taurine 20, dithiothreitol 0.5 supplemented with mitochondrial respiratory substrates, 5 mM glutamate and 2 mM malate; the ionic strength was adjusted to 160 mM with potassium methanesulfonate (total K^+ concentration was 80 mM) and free [Ca^{2+}] was buffered with 10 mM ethylene glycol-bis(β-aminoethyl ether)*N*, *N*, *N*′,*N*′-tetra-acetic acid (EGTA). Then the fibres were stretched in steps of 5% up to the maximum stretch of 30% beyond slack length. This pattern of stretching was repeated in the same solution (control) and in the presence of drugs modulating mitochondrial volume. The passive force per area (mN/mm^2) was calculated for each.

1.2. Estimation of releasable SR Ca^{2+} content *in situ*

To estimate releasable SR Ca^{2+} content *in situ* under different energetic conditions, the fibres were stretched to 120% of their slack length (sarcomere lengths of 2.1–2.2 μm) in the *relaxing solution*. The experimental protocol is shown in Figure 1**.** Each experiment began by equilibrating the fibres in *relaxing solution* in the virtual absence of Ca^{2+}, SR loading was performed for 5 min in *loading solution* at 316 nM Ca^{2+}. After loading, in order to estimate SR Ca^{2+} leakage, the fibres were incubated in *leak solutions* in the absence of Ca^{2+} or at 100 nM Ca^{2+} under different energetic conditions or in the presence of different substances for various periods of time (30–300 s). Excess EGTA was then washed out in *release solution* with 0.2 mM EGTA for 1 min before 5 mM caffeine was added to induce calcium release. The caffeine-induced tension transient was used to calculate the time course of free [Ca^{2+}] close to the myofibrils during release, using the [Ca^{2+}]/tension dependence as an internal calibration. The [Ca^{2+}]/tension relationship was thus measured at the end of each experiment, in the presence of 5 mM caffeine and under conditions identical to those of Ca^{2+} release, except that 10 mM EGTA was present instead of 0.2 mM in order to adequately buffer the free Ca^{2+}. Using this relationship, the [Ca^{2+}] at each step of the tension–time integral was recalculated to obtain [Ca^{2+}]-time integrals (SCa), which were used to evaluate the amount of Ca^{2+} released by the SR.

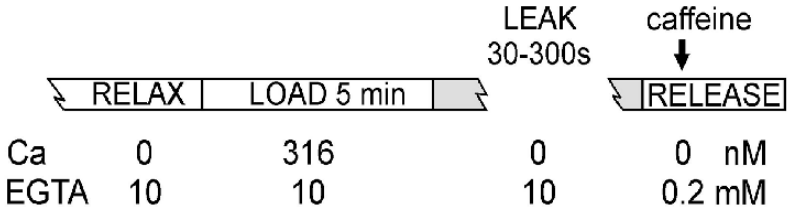

Figure 1. Experimental protocol for leak experiments (see text).

The SR Ca^{2+} uptake in permeabilized fibres was estimated by analysing the the tension transient due to caffeine-induced calcium release after SR loading. The experimental protocol used in this study was a modified version of that described by Minajeva *et al*. (1996). After emptying the SR via a brief application of caffeine (5 mM), the fibres were incubated in *relaxing solution* with or without the experimental substances for 15 min. Then SR loading was carried out in the presence/absence of the same substances in the *loading solutions* at 316 nM Ca^{2+}. After the loading was completed, fresh *relaxing solution* was applied for 30 s and then excess EGTA was washed out in solution with 0.3 mM EGTA for 60 s before 5 mM caffeine was added to induce calcium release.

All solutions were prepared using the *basic solution* containing (in mM) EGTA 10 (except in the release solutions, 0.2), BES 60 (pH 7.1), free Mg^{2+} 1, taurine 20, glutamic acid 5, malic acid 2, K_2HPO_4 3, dithiothreitol 0.5, diadenosine pentaphosphate (P^1,P^5) 0.04 (to inhibit adenylate kinase activity), MgATP 3.16; the ionic strength was adjusted to 160 mM with potassium methanesulfonate. The desired [Ca^{2+}] was obtained by varying the CaK_2EGTA/ K_2EGTA ratio. *Relaxing solution* was made by adding PCr 12 mM. *Loading solution* was the same as the *relaxing solution* but with 316 nM [Ca^{2+}] added. *Leak solutions* were the same as the *basic solution* but additionally contained 2 mM NaN_3 (to inhibit mitochondria) and/or 12 mM PCr (to activate creatine kinase system). In order to study glycolytic support, glycolytic intermediates (4 mM glyceraldehyde-3-phosphate and 4 mM phosphoenolpyruvate) and 4 mM NAD were added to *leak solution* containing ATP and NaN_3. *Release solution* was the same as *relaxing solution* but additionally contained 2 mM NaN_3 and 0.2 or 0.3 mM EGTA (zero Ca^{2+}). All experiments (except where stated) were carried out in the presence of 10 μM RU360, a specific mitochondrial calcium uniporter blocker, in order to avoid any participation of mitochondria in Ca^{2+} fluxes.

2. Preparation of ventricular myocytes

Primary rat and mouse ventricular myocytes were prepared as described earlier by Verde *et al*. (1999). Rat and mouse ventricular myocytes were obtained by retrograde perfusion from hearts of male Wistar rats and male C57BL/6 mice. Briefly, the animals were anaesthetized by intraperitoneal injection of sodium thiopental and the hearts were excised rapidly. The ionic composition of the Ca^{2+}-free Ringer solution was as follows (in mM): NaCl 117, KCl 57, $NaHCO_3$ 4.4, KH_2PO_4 1.5, $MgCl_2$ 1.7, D-glucose 11.7, PCr 10, taurine 20, and HEPES 21, adjusted to pH 7.1 with NaOH at room temperature. For enzymatic dissociation, 1 mg/ml collagenase A (Boehringer Mannhein, Germany) and 300 μM EGTA were added to the Ca^{2+}-free Ringer solution, so that the free Ca^{2+} concentration was adjusted to 20 μM. The hearts were perfused retrogradedly at a constant flow of 6 ml/min and at 37 °C by Ca^{2+}-free solution during 5 min followed by 1 h of perfusion at 4 ml/min with the same solution containing collagenase. The ventricles were then separated from atria, chopped finely and agitated gently to dissociate individual cells. The resulting cell suspension was filtered on gauze and the cells were allowed to settle down. The supernatant was discarded and cells resuspended four more times in Ca^{2+}-free solution containing a progressively increasing calcium concentration. The cells were maintained at 37 °C until use.

3. Preparation of primary culture of cerebellar granule neurons

Primary cultures of cerebellar granule neurons were prepared according to the method of Gallo *et al.* (1982), with slight modifications. Briefly, the cerebelli from 8-day-old Wistar rat pups were dissociated by mild trypsinization (0.25% trypsin at 35 °C for 15 min) followed by trituration in a 0.004% DNase solution containing 0.05% soybean trypsin inhibitor. The cells were resuspended in Eagle's basal medium with Earle's salts (Sigma-Aldrich, Germany) containing 10% heat-inactivated fetal bovine serum, 25 mM KCl, 2 mM glutamine and 100 µg/ml gentamicin. The cell suspension was plated at a density of 1.0×10^6 cells/ml on poly-L-lysine-coated LabTek II chambered cover-glass (0.3 ml/chamber; Nunc, Thermo Fisher Scientific, MA, USA) or at a density of 1.25×10^6 cells/ml on 2 ml poly-L-lysine-coated glass bottom culture dishes (MatTek Corp., MA, USA). 10 µM cytosine arabinoside was added 24 h after plating to prevent the proliferation of glial cells. The cells were cultured for 5–7 days in a humidified 5% CO_2/95% air atmosphere at 37 °C.

4. Preparation of primary culture of cortical neurons

Primary cultures of rat cortical cells were prepared from neonatal Wistar rats. Briefly, cortices were dissected in ice-cold Krebs-Ringer's solution that contained (in mM): NaCl 135, KCl 5, $MgSO_4$ 1, K_2HPO_2 0.4, glucose 15, HEPES 20, pH 7.4 additionally containing 0.3% bovine serum albumine and was trypsinized in 0.8% trypsin for 10 min at 37 ^oC. This was followed by trituration in a 0.008% DNase solution containing 0.05% soybean trypsin inhibitor. Neurons were resuspended in Basal Medium Eagle with Earle's Salts (Sigma-Aldrich) containing 10% heat-inactivated foetal bovine serum, 25 mM KCl, 2 mM glutamine and 100 µg/ml gentamicin and plated onto 35 mm glass-bottom (MatTek) or plastic dishes (Nunc) precoated with poly-L-lysine at a density of 10^6cells/ml (2 ml of cell suspension per dish), or 170 µl per well into clear bottom 96-microwell plates (Nunc). Three hours later the medium was changed to Neurobasal^{TM}-A medium containing a B-27 supplement, 2 mM GlutaMAX^{TM}-I (all solutions from Invitrogen Corp., CA, USA) and 100 µg/ml gentamicin. The cells were cultured in a humidified 5% CO_2/95% air atmosphere at 37 °C.

5. Preparation of GT1-7 culture cells

The GT1-7 hypothalamic neurosecretory cells (Mellon *et al*., 1990.) were maintained in Dulbecco's modified Eagle's Medium (DMEM/F-12, Invitrogen) containing 10% heat-inactivated foetal bovine serum and 100 μg/ml gentamicin. Monolayer cultures at a density of 0.1–0.3 × 10^6 cells/cm^2 were incubated in plastic dishes coated with 0.01% poly-L-lysine and in clear bottom 96-microwell plates (Nunc) in a 5% CO_2/95% air humidified atmosphere at 37 °C. The cells were passaged or used at a confluency of 75–90%. Cells from the fift to fifteenth passages were used for the experiments.

6. Visualization of mitochondria and lysosomes in neurons

For mitochondrial tracking, intact neurons were loaded for 30 min at 37 °C with 100 nM MitoTracker Green or 200 nM MitoTracker Red in culture medium. To stain the cytoplasm, intact neurons were loaded for 30 min with 5 μM CellTracker Green 5-chloromethyl-fluorescein diacetate at 37 °C in Lockey's solution containing (in mM): choline chloride 90, $NaHCO_3$, KCl_2 0.1, KCl 5, $MgCl_2$ 3, HEPES 20 (pH 7.4), glucose 13.6. This solution was replaced with conditioned medium after staining and incubated for a further 30 min before microscopy. For lysosomal staining, the intact cells were loaded for 30 min with 100 nM LysoTracker Red in the culture medium. All dyes were purchased from Invitrogen.

In another set of experiments, the cerebellar neurons were transiently transfected on the second day *in vitro* using Lipofectamine 2000 (Invitrogen) following the manufacturer's protocol. Briefly, 100 μl of OPTI-MEM® (Invitrogen) containing 2% Lipofectamine 2000 and 1 μg of cytosolic-green fluorescent protein DNA (Clontech Laboratories Inc., CA, USA) mixed with either 1 μg of DNA for Lamp1-RFP as the lysosome marker (Sherer *et al*., 2003) or mitochondria-targeted pDsRed2 (mtDsRed2, Clontech) was incubated with ~10^5 cells in glass bottom dishes (MatTek) for 4 h at 37 °C. On completion of incubation conditioned culture medium (Eagle's basal medium, Invitrogen) was added to the cells, and the cells were further grown in humidified 5% CO_2/95% air at 37 °C. The transfected DNAs were allowed to express and accumulate their respective proteins in the targeted organelles for 3 days.

6.1. Three-dimensional analysis of mitochondria

Digital optical sections of 512 × 512 were acquired by a confocal laser scanning microscope (MRC1024, Bio-Rad, Germany) equipped with an Ar-Kr laser (excitation wavelengths 488 and 568 nm) and a ×100 oil immersion objective (1.35 numerical aperture, Olympus, Japan). Voxels were collected at 15 nm lateral and 100 nm axial intervals. Raw images were deconvolved by the AutoDeblur software package (Media Cybernetics, MD, USA). Isosurface three-dimensional pictures were generated using the AutoVisualize software package (AutoQuant Imaging Inc., NY, USA) after binarizing with a fixed 32% threshold value. The details are given in Safiulina *et al.* (2006).

To assure the accuracy of this method, software settings were optimized with green fluorescent microspheres of constant diameter (Molecular Probes PS-Spec Microscope Point Source Kit, Invitrogen). Beads were first bleached with a high laser power in order to receive a similar signal to noise ratio as in mitochondrial preparations, then series of images were recorded with identical parameter setting as used for mitochondrial images. Figure 2 summarizes the data restoration process. Parts A and D depict the projections of raw images in XY and XZ planes and parts B and E show the same images after the data restoration process. Parts C and F show the axial intensity profiles generated from these images and part G presents the final three-dimensional (3D) isosurface picture generated from all slices. The part H shows that the microsphere parameters provided by manufacturer correspond very well with those measured using reconstructed images.

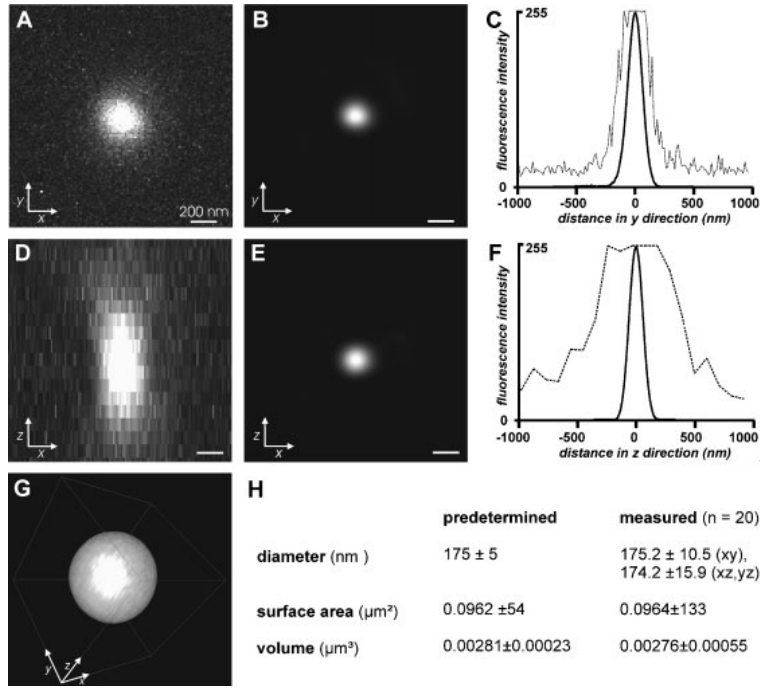

Figure 2. Imaging of subresolution fluorescent microspheres (ø 175 nm). Parts (A and D) show maximal XY and XZ projections of raw image series, respectively. Note the spherical aberration present along the z axis in (D). Parts (B and E) show the maximal XY and XZ projections of 3D deconvolved image series after correction of spherical aberration. Parts (C and F) depict the axial intensity profiles generated from these images before (dotted line) and after (solid line) image restoration. Part (G) shows 3D isosurface reconstruction of the deconvolved image series (frame size 250 × 250 × 250 nm). Part (H) compares the parameters of microspheres provided by the manufacturer with parameters measured from reconstructed images. Note that experimentally determined values correspond well with the manufacturer's values. (Figure from Safiulina *et al*., 2006)

6.2. Quantitative analysis of organelle motility

Organelle motility was measured in intact cultures of cerebellar granule neurons loaded with MitoTracker Green and Lyso-Tracker Red or expressing Lamp1-RFP or mtDsRed2, by time course confocal microscopy. The temperature in the culture medium was kept at 37 °C by a temperature-controlled chamber system, and images were collected using a 40× or 63× spring objective. The pH of the culture medium in the chamber was maintained at pH 7.1 with 20 mM HEPES. The time course analysis was performed using the LaserSharp 2000 software (Bio-Rad) time course option by recording 30 frames with 5 s intervals for one time point. Coordinates of randomly chosen mitochondria were recorded by a

computer and were tracked through the time series. Matrices of the data were further processed using a Microsoft Excel macro which calculated the percentage of time spent in motile state, the distance of displacement, maximal velocity, average velocity, and average velocity in the motile state for each mitochondrion.

7. Visualization of mitochondria and nuclei in cardiomyocytes

To visualize themitochondria the cardiomycytes were loaded for 30 min at room temperature with 200 nM MitoTracker Green. Images were acquired before and after treatment with various mitochondrial modulators for 10–15 min with a LSM 510 META Zeiss confocal microscope (Carl Zeiss Inc., Germany) equipped with Plan-Apochromat 63×/1.4 oil immersion objective using the 488 nm line of an Argon laser for excitation and an LP505 nm filter for detecting emission.

To measure nuclear volume, the nuclei in saponin-permeabilized cardiomyocytes were stained with propidium iodide and further analysed by confocal microscopy. 256 × 256 pixel images were acquired before and after treatment with various mitochondrial modulators using the 543 nm laser line, and the emission was monitored using band pass emission filter (BP 563–660 nm). Voxels were collected at 60–120 nm lateral and 100 nm axial intervals. We minimized the number of zero or saturated pixels while collecting images. Also, only the original raw images were 3D deconvolved and reconstructed using the AutoDeblur and Autovisualize X software package (Media Cybernetics). File names for the acquired images were then encoded to avoid bias and later all images were subjected to morphometric analysis. A grid of points was superimposed on the 2D image sections after what the points that overlaid fluorescent signals were counted. The nuclear volume was then estimated using the Cavalieri principle.

For visualization of nuclear membrane the cardiomyocytes were stained for 15–30 min with 1 μM BODIPY®FL glibenclamide at 37 °C and then visualized using the 488 nm line of an Argon laser for excitation and an LP505 nm filter for detecting emissions.

8. Intra-reticular [Ca^{2+}] monitoring in permeabilized cardiomyocytes, GT1-7 and cortical cells

A low-affinity Ca^{2+} indicator Mag-fluo-4 AM (Invitrogen) trapped within the ER was used to measure luminal free [Ca^{2+}]. Plated mouse/rat cardiomyocytes were loaded with Mag-fluo-4 AM (5 μM) for 45 min at 22 °C, washed with

indicator-free solution and then permeabilized with saponin (50 µg/ml) for 3 min using *basic solution* in the absence of Ca^{2+} (as described in section 1.2 Materials and methods). Cover slips with mouse cells were attached to the stage of a Carl Zeiss LSM-510 confocal microscope with a recording chamber (Warner Instruments, CT, USA). Images were acquired in line scan mode (at intervals 3.5 or 7 ms) along the longitudinal axis of the cell. Intra-reticular [Ca^{2+}] changes in rat cells were monitored by epifluorescence microscopy (NIKON Eclipse TE300, NIKON Instruments Inc., NY, USA) using a standard FITC filter set. The SR Ca^{2+} uptake was monitored at a relatively low extra-reticular [Ca^{2+}] (32 nM) to avoid too rapid and large Ca^{2+} accumulation in the SR leading to a saturation of the indicator. All of the experiments were performed at 22 °C.

To estimate intra-reticular [Ca^{2+}] in GT1-7 and cortical cells in 96-microwell plates (Nunc) the growth medium was removed and the cells were incubated in Krebs-Ringer's solution containing 0.2 mg/ml Pluronic F127 and 5 µM Mag-fluo-4 AM (from a 5 mM stock in anhydrous DMSO) for 40 min at 37 °C. Cells were then permeabilized in Ca^{2+}- free working solution (*basic solution for measuring passive force,* described in section 1.1 Materials and methods), without mitochondrial respiratory substances and containing 50 µg/ml saponin, for 15 min at 4 °C. After permeabilization the solution was changed to fresh working solution supplemented with 2 mM NaN_3 with or without experimental substance and incubated for 30 min at room temperature in the dark. The ER Ca^{2+} measurements were performed with FlexStation™ (Molecular Devices, CA, USA) 475 nm excitation, 495 nm cut-off, and 525 nm emission wave-lengths at room temperature. The Ca^{2+} was added using an automatic pipettor and changes in relative fluorescent units (RFU) were recorded for later analysis.

9. Immunohistochemistry

Isolated cardiomyocytes were fixed with 4% paraformaldehyde in phosphate buffered saline (PBS, 0.1 M, pH 7.4) for 10 min at 37 °C. Cortical cells were fixed with 4% paraformaldehyde solution in growth media in the presence of 5% sucrose for 10 min at 37 °C. After permeabilization as described above the cells were blocked by 10% normal goat serum at room temperature for 60 min and then incubated with primary antibodies at 4 °C overnight. The antibodies used were as follows: rabbit anti-LETM1 (1:250, Atlas Antibodies AB, Sweden), rabbit anti-potassium channel SK_{Ca} (1:200, Sigma-Aldrich, Germany), mouse anti-SERCA2 (1:500, Abcam, USA) and goat anti-cytochrome c oxydase II (1:150, Santa Cruz Biotechnology Inc., Germany). After washing the cells were further incubated with respective fluorochrome conjugated secondary antibodies and examined using confocal microscopy.

10. Separation of ER fraction

Brain cortex from adult mice were homogenized with teflon-glass homogenizer in ice in ice-cold isotonic extraction buffer containing (in mM): HEPES 10 (pH 7.8), sucrose 250, EGTA 1, KCl 25 supplemented with 4% protease inhibitor cocktail (Roche, Germany). Nuclei and cell debris were first removed by centrifugation at 1,000 × *g* for 10 min at 4 °C. Remaining supernatants were then further centrifuged at 12,000 × *g* for 15 min 4 °C after what the mitochondria rich pellet was collected. Remaining supernatant was centrifuged at 55,000 × *g* for 60 min at 4 °C and pellet containing endoplasmic reticulum fraction was suspended in isotonic extraction buffer.

For western blotting the material was lysed in buffer containing (in mM): Tris-Cl 50, ethylenediamine-tetra-acetic acid (EDTA) 1, NaCl 150, Na_3VO_4 1, NaF 1, 1% NP-40, 0.25% sodium deoxycholate and 4% protease inhibitor cocktail (Roche) for 30 min on ice. Equivalent amounts of total protein were separated by SDS-PAGE on 10% or 12% polyacrylamide gels and then transferred to Hybond -P PVDF Transfer Membranes (Amersham Biosciences, UK) in 0.1 M Tris-base, 0.192 M glycine and 10% (w / w) methanol using an electrophoretic transfer system. Further experiment was performed using SNAP i.d. Protein Detection System (Millipore, UK) following the manufacturers guidelines. The membranes were blocked with 0.1% (w / w) Tween-20 in Tris buffered saline (TBS) containing 0.5% (w / w) non-fat dried milk at room temperature for 5 min. After blocking, the membranes were incubated 15–30 min with primary antibodies described earlier (chapter 9. Materials and Methods, antibody dilutions were as follows: anti-LETM1 1:250, anti-potassium channel SK_{Ca} 1:200, anti-SERCA2 1:500, anti-cytochrome c oxydase II 1:150) followed by incubation with appropriate horseradish-peroxidase (HRP)-conjugated secondary antibody (1:400, Pierce, USA) for 20 min at room temperature. Immunoreactive bands detected by enhanced chemiluminescence (ECL, Amersham Biosciences) using medical x-ray film blue (Agfa, Belgium). The blots probed for proteins of interest were densitometrically analyzed using a QuantityOne 710 System (Bio-Rad).

11. Statistical analysis

The values are expressed as mean ± SEM. Statistical differences were determined using one way or repeated measures ANOVA followed by Bonferroni's multiple post *hoc* test and *t*-test or the Mann-Whitney test. $p<0.05$ was accepted as significant in the experiments.

RESULTS

1. Mitochondrial swelling impairs the transport of organelles in cerebellar granule neurons

1.1. Mitochondrial modulators, which affect potassium cation fluxes, modify the mitochondrial morphology

The first aim was to validate the effect of mitochondrial modulators on mitochondrial morphology. It has been previously shown that mitochondrial inhibitors depolarizing the mitochondrial inner membrane considerably increase the mitochondrial size and that this is associated with impaired mitochondrial motility (Safiulina *et al*., 2006). However, compounds inducing mitochondrial depolarization and swelling also de-energize mitochondria and inhibit the production of ATP, which might also account for the loss of mitochondrial motility.

To distinguish between these effects, we decided to use two groups of mitochondrial inhibitors for the current experiments. The first group containing valinomycin (potassium-specific transporter facilitating the movement of potassium ions through lipid membranes "down" an electrochemical potential gradient (Cammann, 1985) and inducing a massive potassium influx into the mitochondrial matrix), antimycin (binds to the Qi site of cytochrome c reductase thereby inhibiting the oxidation of ubiquinol in the electron transport chain of oxidative phosphorylation (Dairaku *et al*., 2004)), and high concentrations of azide (inhibits cytochrome *c* oxidase together with ATP synthetase (Bowler *et al*., 2006 and references therein)), ceases the mitochondrial energy supply to cytoplasmic consumers and produces mitochondrial swelling due to dissipation of the mitochondrial membrane potential. The second group of inhibitors, containing bongkrekic acid (inhibits mitochondrial adenine nucleotide translocase (Henderson and Lardy, 1970), and thus the ATP transport from the mitochondrial matrix to the cytoplasm), and oligomycin (inhibits ATP synthetase (Dairaku *et al*., 2004)), inhibits mitochondrial energy supply to the cytoplasm but does not induce mitochondrial swelling. As can be seen from Figure 3, the inhibitors from the first group, valinomycin, azide and antimycin, induced marked mitochondrial swelling associated with an increase in mitochondrial diameter from 200–300 to 400–600 nm. On the other hand, the inhibitors belonging to the second class, oligomycin and bongkrekic acid, had no effect on mitochondrial morphology (Fig. 3). Thus, although all inhibitors block the ATP-generating activity of mitochondria, only depolarizers induce mitochondrial swelling.

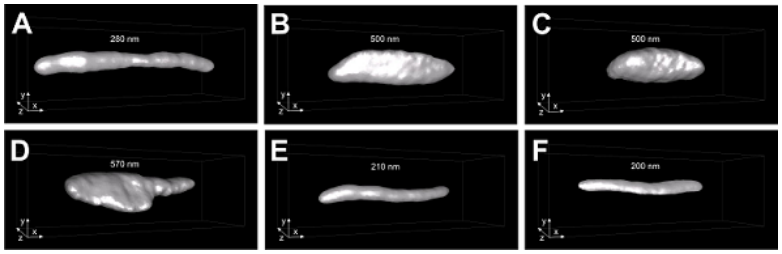

Figure 3. The effect of mitochondrial inhibitors on mitochondrial morphology. 3D reconstructions of a MitoTracker Green stained single mitochondrial from control (A), valinomycin (10 μM, B), azide (25 mM, C), antimycin (100 μM, D), bongkrekic acid (25 μM, E), or oligomycin (50 μM, F)-treated neurons. Each panel shows a 3D isosurface reconstruction of the deconvolved image series (frame size 2.5 × 1.0 × 1.0 μm, l × w × h). Note the increase in the maximal diameter of mitochondria treated with substances that induce membrane depolarizarion (valinomycin, azide, and antimycin).

1.2. Effect of mitochondrial swelling on mitochondrial motility

The next question addressed in the study was whether or not the swelling of mitochondria affects mitochondrial motility in neurons. We measured the mitochondrial motility in the presence of the different classes of mitochondrial modulators. Valinomycin, antimycin, and azide, which induce swelling, almost completely inhibited mitochondrial motility, as demonstrated (Fig. 4) by the decline in average velocity (average distance travelled per second during motile and stationary states) as well as by a fall in duty percentage (percentage of time in the motile state) of individual mitochondria. However, no statistically significant changes in these motility parameters were observed when we treated the neurons with bongkrekic acid or oligomycin. These results demonstrate that inhibition of mitochondrial energy production *per se* cannot be the cause of impaired mitochondrial traffic in neuronal processes. The latter event is instead related to mitochondrial morphology modifications or a drop in mitochondrial membrane potential (the fact, that mitochondrial membrane potential somehow regulates its transportation cannot be excluded) (Safiulina *et al*., 2006).

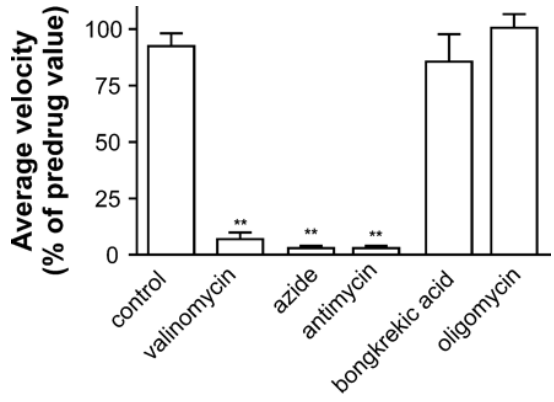

Figure 4. Effect of mitochondrial inhibitors on mitochondrial motility. The figure depicts changes in the average velocity of mitochondria after a 15-min treatment with valinomycin (10 μM), antimycin (100 μM), azide (25 mM), bongkrekic acid (25 μM) and oligomycin (50 μM). The *control* column represents non-treated mitochondria. Each column summarizes data from 4–5 independent experiments and represents at least 100 mitochondria. * different from control at $p < 0.05$, ** different from control at $p < 0.005$.

1.3. Effect of mitochondrial swelling on lysosomal motility

To test whether or not mitochondrial swelling could also block the movement of other organelles, we measured lysosome traffic. Although possibly energy-dependent, lysosome traffic should be independent of the mitochondrial membrane potential itself and should only be impaired in the case when swollen mitochondria mechanically block lysosome passage. The individual experiment depicted in Figure 5 A and C demonstrates that treatment of neurons with valinomycin led to a fast, time-dependent inhibition of lysosomal movement, within a few minutes as estimated by drop in their average speed and duty percentage. At about 10 min after the beginning of the treatment, lysosomal movement almost completely ceased. No decrease in the motility of lysosomes was observed in either control neurons or in bongkrekic acid-treated neurons at any time point after treatment. Figure 5 B and D, showing summarized data of independent experiments, demonstrate that compounds inhibiting mitochondrial movement, valinomycin and azide, inhibited lysosomal movement almost completely when measured 15 min after the start of the drug treatment. Another mitochondrial inhibitor, antimycin, also inhibited the lysosomal traffic, although not as efficiently as the others did. On the other hand, oligomycin (which does not change the mitochondrial geometry), similarly to bongkrekic acid, exerted no inhibitory effect. Rather, on the contrary, lysosomal motility tended to increase in bongkrekic acid-treated neurons. Thus, these data demonstrate that all mitochondrial modulators which induce mitochondrial swelling also inhibit

the organelle transport in the processes of granule neurons and that this effect is not directly related to mitochondrial energy production.

Several observations from our time lapse imaging of the organelles support the "traffic jam" hypothesis. Swollen mitochondria are often localized near lysosomes, and the effect of mitochondrial swelling on lysosome transport is dependent on the diameter of neurites. Average velocity of lysosomes in thin processes is almost zero when the culture is treated with valinomycin (10μM), whereas in thick processes the average velocity is decreased only by about 50% of the control value (p<0.05 when comparing the thin versus thick neurites). Thus, these observations suggest that steric hindrance of swollen mitochondria rather than the mitochondrial membrane potential itself or energy drop could be the major factor behind the ceased organelle movement.

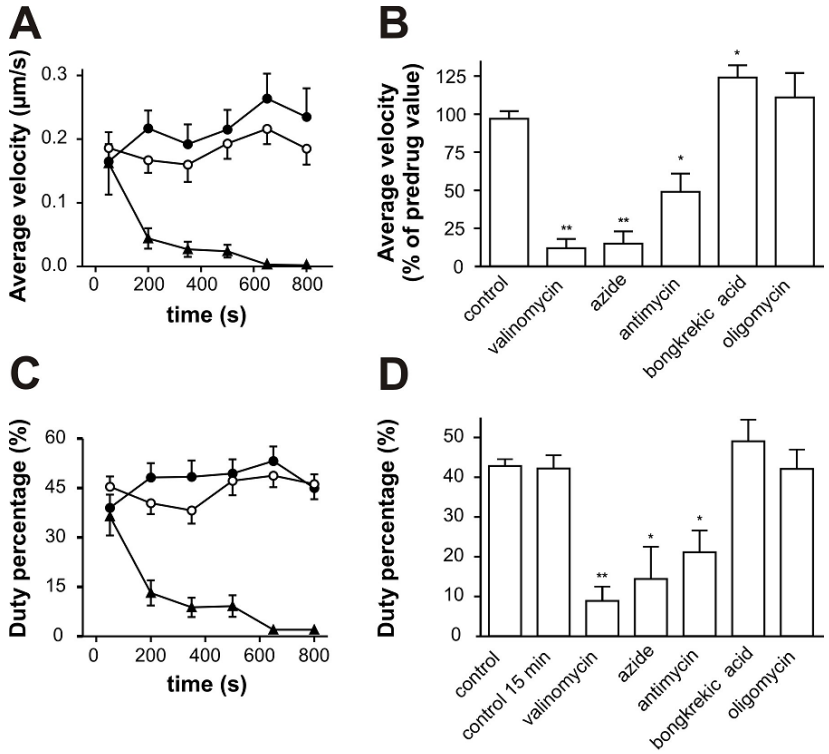

Figure 5. Effect of mitochondrial inhibitors on lysosomal motility. (A and C) depict the data from single experiment where neurons where treated with valinomycin (10 μM, *closed triangles*) or bongkrekic acid (50 μM, *closed circles*) when compared with untreated control (*open circles*). The figure shows time-dependent changes in average velocity (A) and in duty percentage (C) of lysosomes (each data point represents 25–50 lysosomes). (B and D) demonstrate changes in average velocity and in duty percentage of lysosomes after a 15-min treatment with valinomycin, azide (25 mM), antimycin (100 μM), bongkrekic acid (25 μM), or oligomycin (50 μM). Each column summarizes data from 4–5 independent experiments and represents at least 100 lysosomes. * different from control at $p < 0.05$, ** different from control at $p < 0.005$.

2. Swollen mitochondria as sources of intracellular mechanical signalling

2.1. Passive force as a sensor of compression of the myofibrillar compartment in cardiac fibres

In order to estimate intracellular compression, we measured the passive force developed by saponin-permeabilized fibres. The passive characteristics (passive force and stiffness) of cardiac myofilaments are known to be very sensitive to mechanical compression associated with a decrease in lattice spacing (Martyn *et al*., 2004; Roos and Brady, 1990). We first tested whether or not passive force responds to compression of the myofibrillar compartment. Figure 6 shows that after stretching under control conditions, there was an increase in passive force when permeabilized fibres underwent stepwise lengthening in the presence of

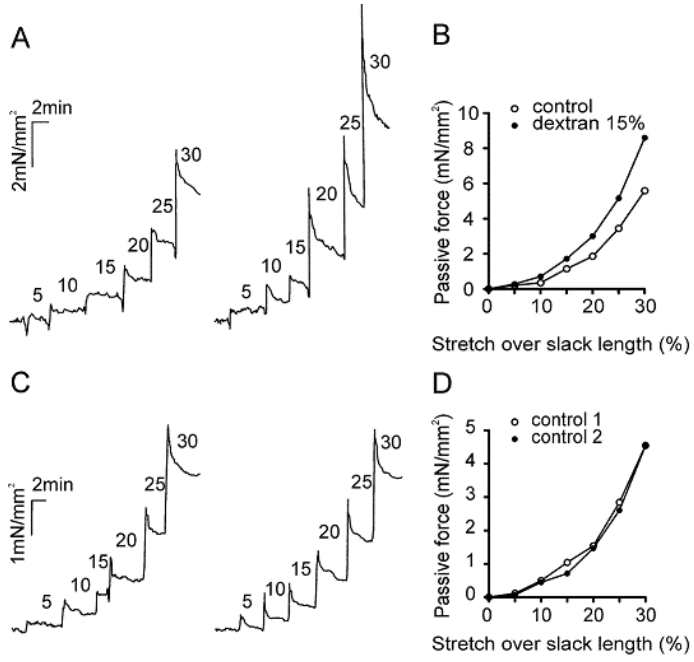

Figure 6. Effect of 15% dextran on the passive force developed by permeabilized ventricular fibres. (A and C) Traces of a typical experiment showing the increase in passive force following fibre stretch. Numbers indicate the percentage augmentation in fibre length beyond slack length. The first cycle of stretch in the absence of dextran was followed by a second cycle of stretch in the presence (A) or in the absence (C) of dextran. (B and D) Plots showing passive force as a function of fibre stretch for the experiments is shown in (A) and (C), respectively. Note, that panels (B) and (D) represent results from single experiments.

15% dextran (osmotic pressure 46 kPa). In contrast, there was no difference in passive tension when permeabilized fibres underwent two consecutive cycles of passive stretch under the same control conditions. These results confirm that the induction of passive force by myofibrillar compression can be used as a sensor for intracellular tension.

2.2. Swelling of the mitochondrial matrix increases cardiac fibre passive force

Increase in mitochondrial volume was achieved using ion channel-forming peptide alamethicin (Bechinger, 1997) or inhibitor of KHE propranolol (also known to block K_{ATP} channel on cell membrane (Xie *et al*., 1998)), which are known to cause matrix swelling. Confocal microscopy of cardiomyocytes after incubation with both substances revealed considerable augmentation of mitochondrial size (Fig. 7 A, B, C and D upper panels). Spaces between the mitochondria disappeared and distances between mitochondrial rows became shorter because of the greater volume of the mitochondria. Mitochondrial volume was measured before and after treatment with propranolol. On the basis of the 3D images, we estimate that propranolol increased mitochondrial volume from ~1.88 ± 0.16 μm^3 (n = 17) to 3.04 ± 0.17 μm^3 (n = 17, $p < 0.001$).

We further studied whether or not such mitochondrial swelling is able to change the mechanical properties of fibres. We found that incubation of permeabilized fibres with alamethicin or propranolol indeed significantly increased passive force. As can be seen in Figure 7, increases in relaxed fibre length induced a much higher force when the mitochondria were swollen.

In the next series of experiments, we studied the effects of diazoxide, a mitochondrial ATP-sensitive potassium channel opener known to cause moderate mitochondrial swelling by inducing potassium accumulation in the matrix. Diazoxide treatment mainly increased the passive force at moderate lengths of stretch; at 10% stretch, the force was augmented by 28 ± 5%. The solvent DMSO had no significant effect. On the other hand, 5-HD, a putative specific inhibitor of ATP-sensitive mitochondrial potassium channels, completely blocked the effect of diazoxide, confirming the role of channel opening in mediating diazoxide's effect on passive force. Altogether, these experiments show that mitochondrial swelling has a marked impact on the mechanical properties of cardiomyocytes.

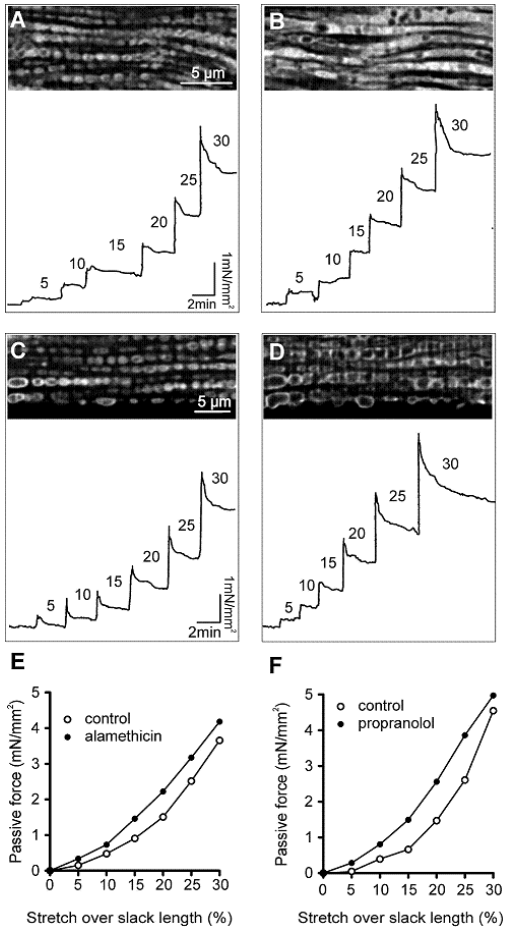

Figure 7. Effects of drugs inducing mitochondrial swelling on passive force development by permeabilized ventricular fibres. (A–D) Upper panels—confocal images of cardiomyocytes before (A and C) and after addition of alamethicin (10 µg/mL, B) or propranolol (1 mM, D). Lower panels—traces of typical experiments showing the increase in passive force following fibre stretch. Numbers indicate the percentage augmentation in fibre length beyond slack length. (E and F) Plots showing passive force as a function of fibre stretch in the presence of alamethicin (E) or propranolol (F). Note, that panels (E) and (F) represent results from single experiments.

2.3. Nuclear volume as a sensor of intracellular mechanical interactions

In this series of experiments, we estimated to what extent nuclear geometry is sensitive to intracellular pressure. In order to increase pressure on the nuclear envelope, we used 70 kDa dextran, which is too large to cross nuclear pores. Figure 8 A-C is a 3D reconstruction of nuclei showing that significant changes in nuclear morphology occurred when the concentration of dextran was increased from 0 to 6% or 15%. Figure 8 D shows that the dextran-induced increase in osmotic pressure is inversely related to nuclear volume. These experiments further show that nuclear volume can serve a fine sensor for detecting intracellular pressure.

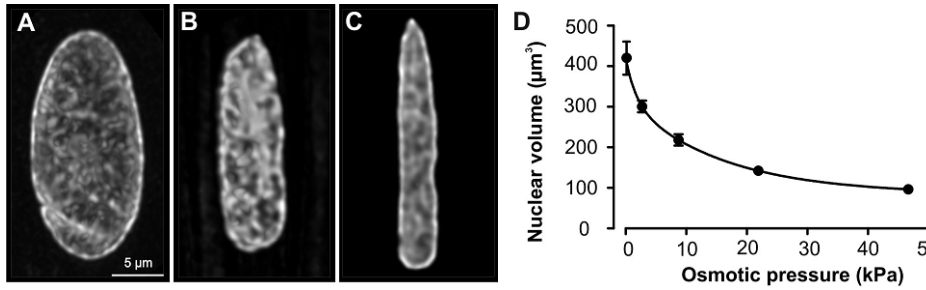

Figure 8. Osmotic pressure compresses nuclei (A-C). Confocal images of nuclei under different osmotic pressures (A, without dextran; B and C, in the presence of 6 and 15% dextran, respectively). (D) Calculated nuclear volume as a function of osmotic pressure in the incubating medium.

2.4. Swelling of the mitochondrial matrix decreases nuclear volume

We next determined whether or not mitochondria can increase the intracellular pressure enough to alter nuclear morphology. Figure 9 A–C shows that both alamethicin and propranolol induced significant mitochondrial swelling that completely changes the geometry of nuclei. The surface area of sections through the nuclei was considerably reduced. The normal convex form of the nuclei was lost due to compression by swollen mitochondria. The 3D reconstructions of these nuclei (Fig. 9 D–F) demonstrate that this was not only associated with remodeling of nuclear shape but also with nuclear compression.

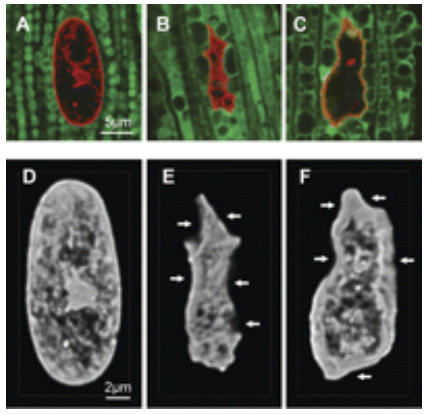

Figure 9. Mitochondrial swelling compresses nuclei. (A–C) Confocal images of cardiac fibres in control (A) and in the presence of alamethicin (10 µg/mL, B) or propranolol (500 µM, C). (D–F) 3D images of nuclei in control (D) and in the presence of alamethicin (E) or propranolol (F). Arrows indicate sites of deformation produced by swollen mitochondria.

In the next series of experiments, we studied the effects of more moderate mitochondrial swelling induced by two drugs which cause potassium accumulation in the matrix: valinomycin and diazoxide. Nuclear volume was calculated using 3D reconstructed confocal images, allowing us to precisely

estimate nuclear volume before and after incubation in the presence of the drugs. The pressure that induced nuclear compression was calculated using a calibration curve obtained with dextran. Figure 10 A, B shows that incubation of permeabilized cardiomyocytes with both substances (separately) led to a significant reduction in nuclear volume (by 12 ± 2%). Importantly, 5-HD, a putative specific inhibitor of K_{ATP}, completely blocked the effect of diazoxide (Fig. 10 B). Figure 10 C and D shows that the pressures exerted on the nucleus in the presence of valinomycin or diazoxide are approximately 2 kPa. In order to exclude the possibility that this decrease was due to the inhibition of mitochondrial ATP-generating activity, we treated permeabilized cells with bongkrekic acid, an adenine nucleotide translocator blocker that does not alter matrix volume (Kaasik *et al*., 2004; Safiulina *et al*., 2006). Inhibition of ADP phosphorylation without mitochondrial swelling did not change the nuclear volume (Fig. 10 A).

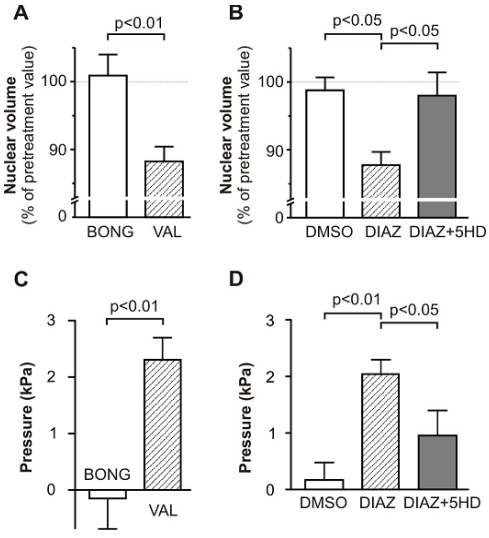

Figure 10. Valinomycin and diazoxide decrease nuclear volume. (A) Effect of 10 μM valinomycin on nuclear volume where 25 μM bongkrekic acid was used as a negative control. (B) Effect of 150 μM diazoxide and 150 μM 5-HD on nuclear volume. (C and D) Calculated pressure exerted on nuclei in the presence of valinomycin (C) or diazoxide (D).

3. Endoplasmic reticulum potassium and proton fluxes govern SR/ER calcium uptake

3.1. Potassium is required for ER calcium uptake

It is well known that SERCA activity is regulated by some ER membrane proteins (phospholamban or sarcolipin), by its substrates and products (beside Ca^{2+} itself also the ATP/ADP ratio close to its vicinity) and by counter-ion movements, as well. The aim of the following experiments was to clarify whether or not and to what extent could ER potassium and proton fluxes control ER Ca^{2+} uptake.

ER Ca^{2+} uptake was measured in two different preparations using two independent methods: in saponin permeabilized immortalized hypothalamic neurons (GT1-7 neurons) and primary cortical neurons using the Mag-fluo-4 AM fluorescent indicator and in permeabilized cardiac fibres using caffeine-induced calcium release method. To study the relevance of potassium ions in Ca^{2+} uptake we first completely replaced the potassium ions in the uptake solution with sodium ions or with tetraethylammonium ions (TEA^+), also known to block potassium channels non-selectively. Both forms of replacement led to the strong inhibition of Ca^{2+} uptake in GT1-7 neurons (Fig. 11 A, B). Replacement of potassium with TEA^+ also inhibited SR Ca^{2+} uptake in permeabilized cardiac fibres (Fig. 11 C). Thus, we can conclude that potassium is essential for ER Ca^{2+} uptake.

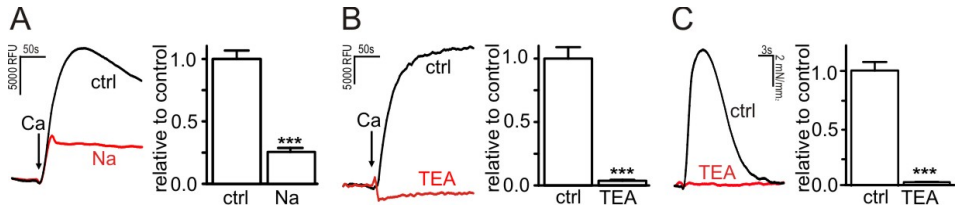

Figure 11. Replacement of K^+ with Na^+ or TEA^+ inhibit *in situ* ER Ca^{2+} uptake. (A and B) Time course of luminal Ca^{2+}-dependent fluorescence after Ca^{2+} addition (left panels) and mean values of maximal fluorescence (right panels) in GT1-7 neurons in the presence of Na^+ (A) or TEA^+ (B) as compared with control conditions (ctrl) in the presence of physiological K^+ concentrations. (C) Force transients in ventricular permeabilized fibres elicited by 5 mM caffeine after 5 minutes of SR Ca^{2+} loading in the presence of K^+ or TEA^+ (left panels) and mean values of tension-time integrals (right panels).

3.2. K_{Ca} but not K_{ATP} channels are involved in ER calcium uptake

In order to find out which potassium channels are required for proper ER Ca^{2+} uptake, we studied the effects inhibitors of different potassium channels had on ER Ca^{2+} uptake. Inhibitors of K_{ATP} channels, 5-HD and glimepiride did not show any effect on ER Ca^{2+} uptake in GT1-7 neurons (Fig. 12), primary cortical neurons and cardiac fibres (data not shown). Note no effect was observed when activators of K_{ATP} channels, diazoxide and pinacidil were used either.

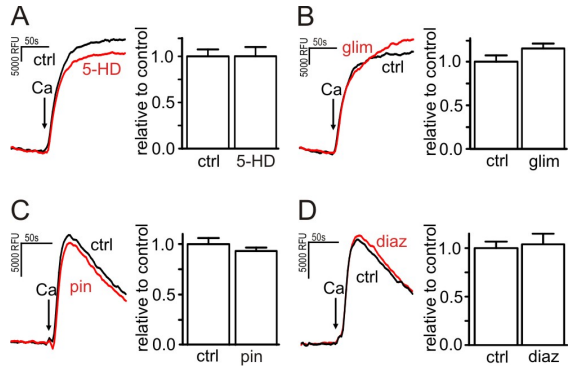

Figure 12. Inhibitors of K_{ATP} channels, 5-HD (100 µM, A) and glimepiride (50 µM, B), as well as K_{ATP} channel openers pinacidil (200 µM, C) and diazoxide (150 µM, D) had no effect on ER Ca^{2+} uptake in GT1-7 neurons. Time course of luminal Ca^{2+}-dependent fluorescence after Ca^{2+} addition (left panels) and mean values of maximal fluorescence (right panels) are shown.

On the other hand, inhibitors of SK_{Ca} channels, UCL 1684 and dequalinium, inhibited ER Ca^{2+} uptake in all preparation: GT1-7 neurons, primary cortical neurons and cardiac fibres as shown in Figure 13. Charybdotoxin (200nM, an inhibitor of BK_{Ca} channels) and TRAM 34 (10 µM, an inhibitor of IK_{Ca} channels) had no inhibitory effect on GT1-7 cells. Furthermore, activators of SK_{Ca} channels, DC-EBIO (50 µM) and NS 309 (50 µM), had no strong effect on Ca^{2+} uptake (data not shown). This data suggest that SK_{Ca} but not K_{ATP} channels control the potassium fluxes required for efficient ER Ca^{2+} uptake.

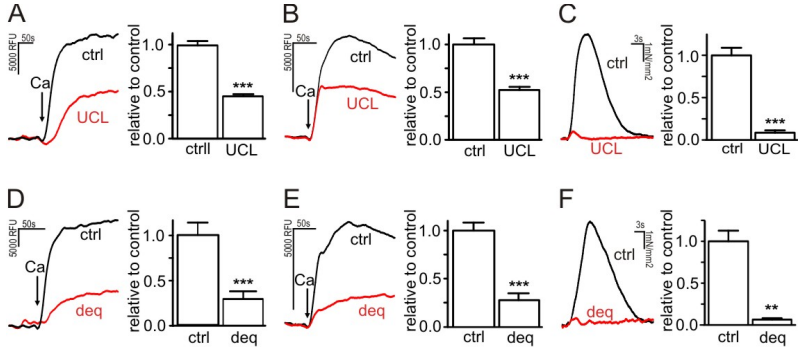

Figure 13. Inhibitors of SK_{Ca} channels, UCL 1684 (50 µM) and dequalinum (100 µM) inhibit ER Ca^{2+} uptake. Time course of luminal Ca^{2+}-dependent fluorescence after Ca^{2+} addition (left panels) and mean values of maximal fluorescence (right panels) in GT1-7 neurons (A, D) or in primary cortical neurons (B,E) in the presence of UCL 1684 (A and B) or dequalinum (D and E) as compared with control conditions (ctrl). Force transients in ventricular permeabilized fibres elicited by 5 mM caffeine after 5 minutes of SR Ca^{2+} loading in the presence of UCL 1684 (C) or dequalinum (F) (left panels) and mean values of tension-time integrals (right panels).

3.3. KHE is involved in ER calcium uptake

ER cation fluxes could be also governed by KHE or NHE. In order to study the role of these exchangers, we investigated the effects of KHE inhibitors, propranolol and quinine, as well as a NHE inhibitor, cariporide, on ER Ca^{2+} uptake. Propranolol and quinine, but not cariporide, blocked ER Ca^{2+} uptake (Fig. 14). It is also interesting to note that in the cardiac fibres we were able to partially reverse the blocking effect of propranolol with an externally added KHE exchanger, nigericin (Fig. 14 D). Thus, KHE is involved in the regulation of ER Ca^{2+} uptake.

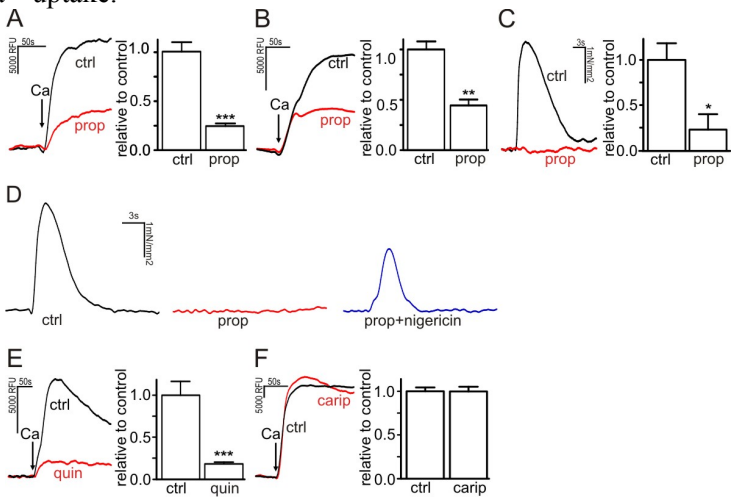

Figure 14. Propranolol (500 µM) inhibited ER Ca^{2+} uptake in GT1-7 neurons (A), primary cortical neurons (B) and cardiac fibers (C). The inhibitory effect of propranolol on cardiac fibres was reversed by nigericin (30 µM, D). Quinine (500 µM, E), but not cariporide (50 µM, F), had an inhibitory effect on GT1-7 neurons.

3.4. SK_{Ca} channels and KHE are expressed in ER

Our next aim was to test whether or not abovementioned potassium channels, as well as KHE, are present in ER membranes. The K_{ATP} channels were visualized using a green fluorescent probe BODIPY®FL glibenclamide and the SK_{Ca} channels with a specific antibody. The ER was visualized using fluorescent thapsigargin which is able to bind to SERCA in living cells or the antibody against SERCA2. As shown (Fig. 15), both K_{ATP} and SK_{Ca} channels are located also intracellularly in primary cortical neurons. The SK_{Ca} channels and in lesser extent K_{ATP} channels are colocalizing with the ER marker. Moreover, also 3D analysis of colocalizations demonstrated that SK_{Ca} channels had also intracellular location. SK_{Ca} channels are showed reticular like staining in cardiomyocytes (Fig. 16) and they were also present in the purified ER fraction, as demonstrated by Western blot analysis (Fig. 17).

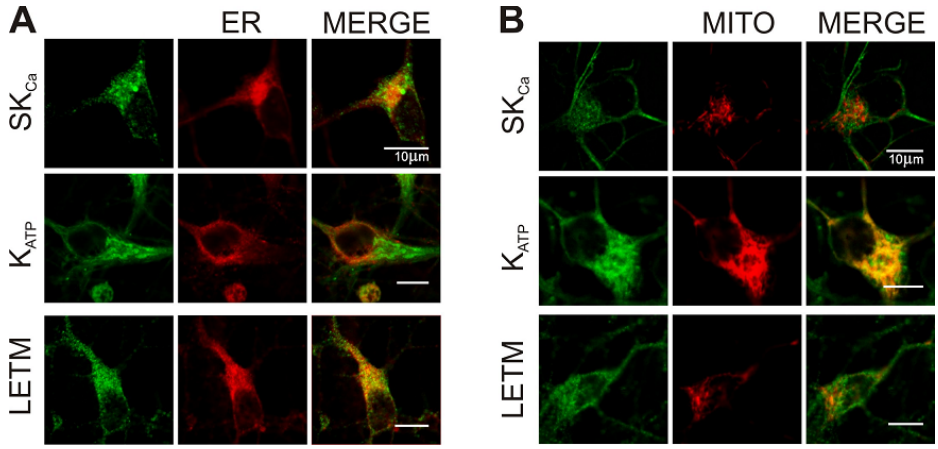

Figure 15. Imaging of SK_{Ca} and K_{ATP} channels and LETM1 in cortical neurons. Panel (A) demonstrates that antibody stainings of SK_{Ca} and anti-LETM1 but not K_{ATP} staining (glibenclamide-BODIPY®FL) colocalize with the ER marker (anti-SERCA2). Panel (B) shows that SK_{Ca} and LETM1 do not colocalize with mitochondria (mitochondrial pDsRed2).

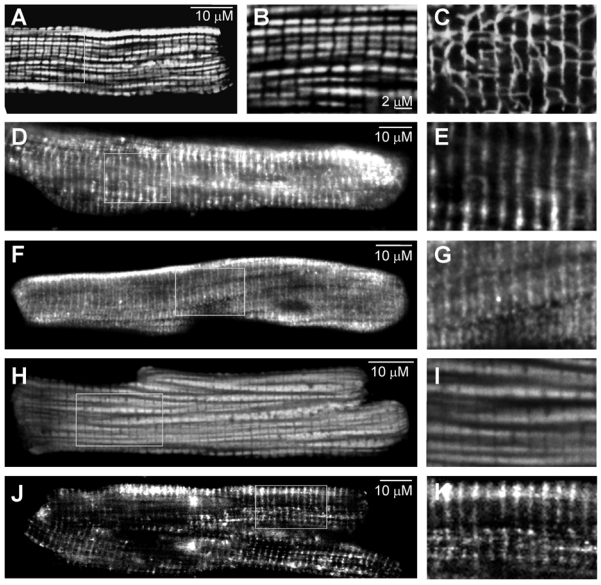

Figure 16. Imaging of SK_{Ca} and K_{ATP} channels and LETM 1 in cardiomyocytes. Panel (A) demonstrates the mitochondrial signal (Mitotracker Green, zoom in B), (C) T-tubules (DiOC16) and (D) sarcoplasmic reticulum marker (anti-SERCA2, zoom in E). The antibody staining pattern of SK_{Ca} (panel F and zoom in G) cannot be attributed only to mitochondria or T-tubules but mostly to sarcoplasmic reticulum. K_{ATP} signal (glibenclamide BODIPY®FL) is mostly mitochondrial (H and zoom in I) and antibody staining of LETM1 is mostly from the sarcoplasmic reticulum (J and zoom in K).

It has been recently shown that mitochondrial KHE is coded by the *LETM1* gene. LETM1 has N-terminal mitochondrial targeting sequence but also an endoplasmic reticulum membrane sequence site in its C-terminus. We therefore checked the localization of LETM1 using a specific antibody. As demonstrated in Figures 15 and 16 LETM1 was colocalized with the ER in both cortical neurons and cardiomyocytes and LETM1 was also present in the purified ER fraction, as demonstrated by Western blot (Fig. 17).

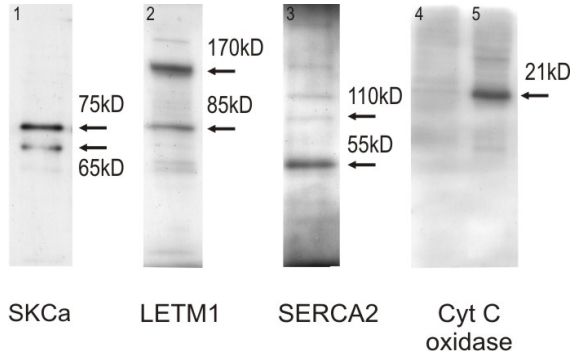

Figure 17. Western blot analysis showing the presence of SK_{Ca} (line 1) and LETM1 (line 2) in the ER fraction purified from the brain. Note that the ER fraction is rich in SERCA2 (line 3) but free of mitochondrial contamination of cytochrome c oxidase (line 4 and line 5 where the mitochondria-enriched fraction was used as a positive control).

4. Energetic state is a strong regulator of SR calcium loss in cardiac muscle: different efficiencies of different energy sources

4.1. Demonstration of SR calcium loss *in situ*

This part of the work started with a series of experiments aimed at finding out whetheror not SR Ca^{2+} loss exists under conditions of a high intra/extrareticular Ca^{2+} gradient *in situ*. Existence of Ca^{2+} loss from the SR was tested using intra-reticular [Ca^{2+}] monitoring of permeabilized cardiomyocytes loaded with the Ca^{2+} sensitive dye Mag-fluo-4 AM. Incubation of cardiomyocytes at 32 nM Ca^{2+} induced an accumulation of Ca^{2+} in the SR while removal of Ca^{2+} from the external medium led to a rapid decrease in intrareticular [Ca^{2+}], which proved the existence of a Ca^{2+} leak. This leak was significantly accelerated if the energy supply was reduced by withdrawing phosphocreatine, e.g changing the local energetic conditions.

In the next series of experiments, the time course of the decrease in the amount of releasable Ca^{2+} in permeabilized cardiac fibres was investigated. The

protocol is shown in Figure 1. The SR in permeabilized mouse ventricular fibres was loaded at 316 nM Ca^{2+} for 5 min under optimal energetic conditions, i.e. in the presence of 12 mM PCr (to activate the creatine kinase supported ATP supply) and activated mitochondria. Afterwards, Ca^{2+} was washed out with the *leak solution* for 30 s, also under optimal energetic conditions, and then the fibres were incubated for 1 min in *release solution* (in order to wash out the high levels of EGTA). Finally, 5 mM caffeine was applied to induce release of the sequestered Ca^{2+}, which elicited a relatively high tension transient (Fig. 18 A). Peak tension was about 75% of the maximum Ca^{2+}-induced force. However, as the duration of incubation in *leak solution* increased, the caffeine-induced tension transient progressively declined (Fig. 18 A). This was not related to a run-down of the fibre state because at the end of the experiment the tension transient was still as high as it was at the beginning. Thus, in permeabilized fibres in the absence of extra-reticular Ca^{2+}**,** the SR *in situ* progressively loses internal Ca^{2+}.

It has previously been shown that in the absence of both active creatine kinase (CK) and mitochondrial function, "cytosolic" ATP, even at a high concentration, is a poor substrate for cellular ATPases. Here, under the same energetic conditions, i.e. with ATP as the sole energy source we found that the Ca^{2+} leak was markedly increased. Figure 18 B shows that when the energy support is compromised, 5 min incubation in the absence of Ca^{2+} leads to an almost complete exhaustion of intra-SR releasable Ca^{2+}.

Figure 18 C shows the Ca^{2+}-time integral values (SCa) for caffeine-induced transients normalized to the maximal SCa values obtained after the shortest duration of leak (30s) for the same fibre. It can be seen that in the absence of mitochondrial and CK support, SR loses Ca^{2+} about two fold faster than under optimal energetic conditions. Thus, altogether these data suggest that Ca^{2+} loss from the SR depends on the energetic condition.

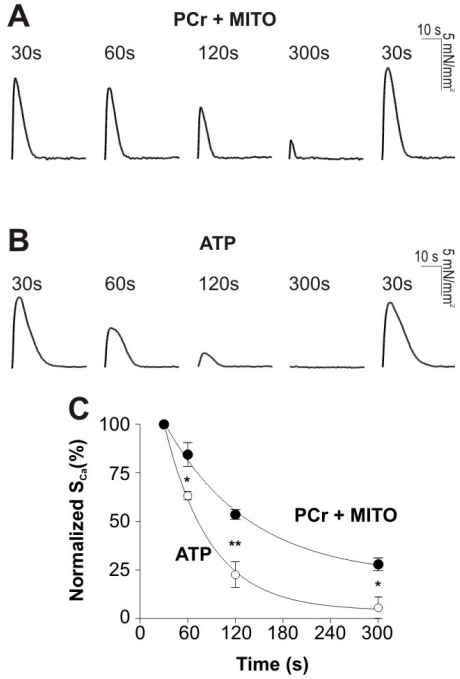

Figure 18. Evidence for energy-dependent SR Ca^{2+} loss. (A and B) Force transients elicited by 5 mM caffeine after 5 minutes of SR Ca^{2+} loading under optimal energetic conditions followed by 30–300 s incubation in *leak solution*. Note that each cycle was preceded by standard SR Ca^{2+} loading under optimal energetic conditions. (A) *Leak solution* contained 3.16 mM MgATP + 12 mM PCr in the absence of mitochondrial inhibitor (PCr + MITO, optimal energetic conditions). (B) *Leak solution* contained 3.16 mM MgATP in the absence of PCr and in the presence of 2 mM NaN_3 to inhibit mitochondria (ATP only). (C) Calcium-time integrals (SCa) for caffeine-induced transients in the presence of PCr and working mitochondria (optimal energetic conditions, filled circles, n=4) or ATP alone (open circles, n=3). For each fibre, SCa values were normalized to SCa obtained after the shortest (30 s) leak Experimental points were fitted using a monoexponential decay function. * $p<0.05$, ** $p< 0.01$ between two conditions, *t*-test.

4.2. Effects of the SERCA and RyR inhibitors

There are two hypothetical pathways by which Ca^{2+} loss from the SR may occur: a passive leak via the RyR and a Ca^{2+} pump-mediated backward flux. To determine the relative contribution of each, we studied the effects of SERCA and RyR inhibitors on Ca^{2+} loss.

As already shown, the SR looses almost all of its Ca^{2+} after 5 min incubation in leak solution without CK and mitochondrial energetic support. Adding the inhibitors of SERCA, CPA and TBQ, into the *leak solution* (where the only

energetic support was "cytosolic" ATP) increased the caffeine-induced force transient after 5 min incubation without Ca^{2+} largely (Fig. 19). We estimated the amount of released Ca^{2+} after incubation in the *leak solution* by normalizing the [Ca^{2+}] -time integral of the caffeine-induced transient to the maximal [Ca^{2+}] -time integral obtained after the shortest (30 s) incubation of the same fibre. Figure 19 C shows that 5 min incubation without Ca^{2+} led to the loss of about 90% of the SR calcium, whereas after Ca^{2+} pump inhibition by CPA, the SR still retained about 50% of its initial calcium content. It should be noted that both, CPA and TBQ, were unable to completely inhibit SERCA under our experimental conditions, which could explain their limited efficiency in the inhibition of SR Ca^{2+} loss.

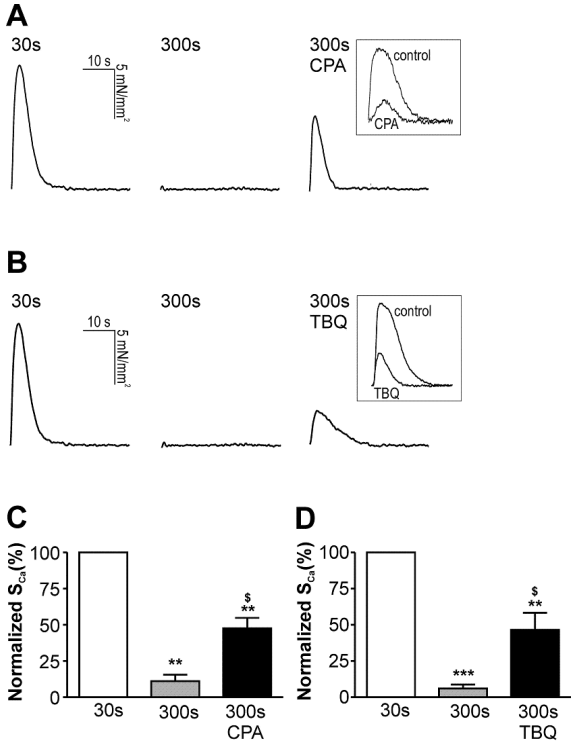

Figure 19. Inhibition of the Ca^{2+} pump decreases SR Ca^{2+} loss. (A and B) Force transients elicited by 5 mM caffeine after different leak protocols. The same fibres were subjected to consecutive cycles of 5 min SR Ca^{2+} loading, each followed by incubation in *leak solution* for various durations – 30 s, 300 s, or 300 s, with or without CPA (150 μM, A) or TBQ (10 μM, B) in the presence of ATP only. Inserts depict force transients elicited by caffeine just after 5 min SR Ca^{2+} loading in the presence or absence CPA or TBQ. (C and D) Normalized SCa values of caffeine-induced transients for CPA (C) or TBQ (D). ** $p<0.01$, *** $p<0.001$ (n =3 for CPA experiments, n=4 for TBQ experiments) vs SCa obtained after 30s incubation in *leak solution* (taken as 100%). $ $p<0.05$ vs normalized SCa in the absence of SERCA inhibitors.

In the next series of experiments (Fig. 20), we asked whether RyR inhibition was able to 'rescue' intra-SR calcium. After SR loading, the fibres were incubated in leak solution in the presence of 1 mM tetracaine, a blocker of the RyR. As for other series, this incubation was followed by a 1 min exposure to release solution in order to wash out the high EGTA concentration. This solution did not contain tetracaine, thus this compound was withdrawn before caffeine challenge. We found that tetracaine was not able to block Ca^{2+} leak such that there was insufficient intra-SR Ca^{2+} to produce a caffeine-induced force transient (Fig. 20 A). Averaged, normalized Ca^{2+}-time integral values for caffeine-induced transients (Fig. 20 C) show the inability of tetracaine to inhibit Ca^{2+} leak in the absence of extra-reticular calcium. In presence of mitochondrial Ca^{2+} uniporter ruthenium red (RR) that has been shown to inhibit also RyR (Xu *et al*., 1999) Ca^{2+} loss was not inhibited (Fig. 20 B and D).

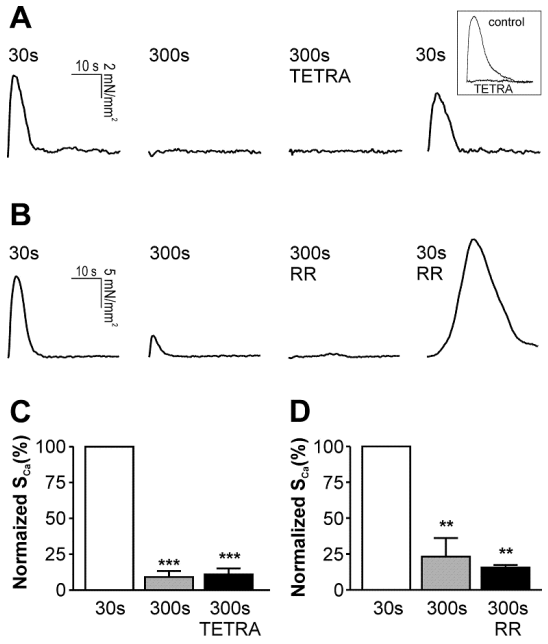

Figure 20. RyR inhibition does not influence SR Ca^{2+} leak. (A and B) Force transients elicited by 5 mM caffeine after different leak protocols. The same fibres were subjected to cycles of 5 min SR Ca^{2+} loading, each followed by incubation in *leak solution* for various durations – 30 s, 300 s, or 300 s, with or without tetracaine (1 mM, A) or RR (10 μM, B) in the presence of ATP only. The last tension transient was obtained in the same fibres in the absence of tetracaine or RR to verify that no run-down of the fibres had occured. Insert to panel (A) shows that 1 mM tetracaine added to *release solution* blocks Ca^{2+} release elicited by 2 mM caffeine (positive control). Note that RR was added after eliciting caffeine-induced transients in the absence of RR and then was continuously present in all solutions. Normalized SCa values of caffeine-induced transients for tetracaine (C) or RR (D). ** $p<0.01$, *** $p<0.001$ (n =3 for each series) vs SCa obtained after 30s incubation in *leak solution* (taken as 100%).

4.3. Efficiency of different energy sources in inhibiting the backward SR calcium leak

Five different energetic pathways, to inhibit Ca^{2+} leak via SERCA in a Ca^{2+}-free medium, were compared. These pathways were: (I) ATP only, (II) glycolytic support; (III) mitochondrial support; (IV) CK support, and (V) optimal energetic conditions (mitochondrial and CK support). Caffeine-induced [Ca^{2+}]-time integrals recorded after 5 min incubation of the permeabilized fibres in the *leak solution* were normalized to corresponding values obtained in the same fibre under optimal energetic conditions (Fig. 21). The efficacy of "cytosolic" ATP and the production of ATP by endogenous glycolytic enzymes bound to intracellular structures in inhibiting the Ca^{2+} leak were very low. Working mitochondria inhibited the backward SR Ca^{2+} leak three to four times more than exogenous ATP as the only energy source. Interestingly, the CK-mediated inhibition of the Ca^{2+} backward flux was markedly more efficient than with ATP alone or with glycolytic support, but it was significantly less efficient than the effect of mitochondrial activity although the differences between the CK and mitochondrial energetic supports did not reach statistical significance. Taken altogether, these data show that different energy sources have very different capacities for inhibiting the Ca^{2+} pump-mediated Ca^{2+} leak.

Qualitatively similar results were obtained in the experiments on isolated cardiomyocytes where intra-reticular [Ca^{2+}] was monitored using the fluorescent indicator Mag-fluo-4 AM (for more detailed information, see in publication number 2 "Energetic state is a strong regulator of sarcoplasmic reticulum Ca^{2+} loss in cardiac muscle: different efficiencies of different energy sources").

According to the fact that although RyR openings are induced by cytosolic Ca^{2+} but our leak experiments were made in the presence of a high concentration of Ca^{2+} buffer and in the virtual absence of cytosolic Ca^{2+}, which might have influenced our results, we performed additional experiments in order to determine whether or not the Ca^{2+} loss was also energy-dependent at a physiological Ca^{2+} concentration. Therefore, after loading the fibres they were incubated in the *leak solution* at [Ca^{2+}] 316 nM, which is close to the physiological concentration, under different energetic conditions: in optimal energetic conditions (in the presence of PCr, external ATP and working mitochondria) and in the weakest energetic conditions (external ATP only) in *leak solution*. Experiments were performed in the presence or absence of tetracaine (blocker of RyR) in order to distinguish the leak through RyR. An important role of the backward Ca^{2+} flux in SR Ca^{2+} loss at a low intracellular [Ca^{2+}] was revealed.

Altogether these results show that at low extra-reticular Ca^{2+} concentration, the backward SR flux strongly depends on the energy state of the cell and the main inhibitor of this Ca^{2+} loss is energy channeling between the mitochondria and SERCA rather than CK-catalyzed energy support.

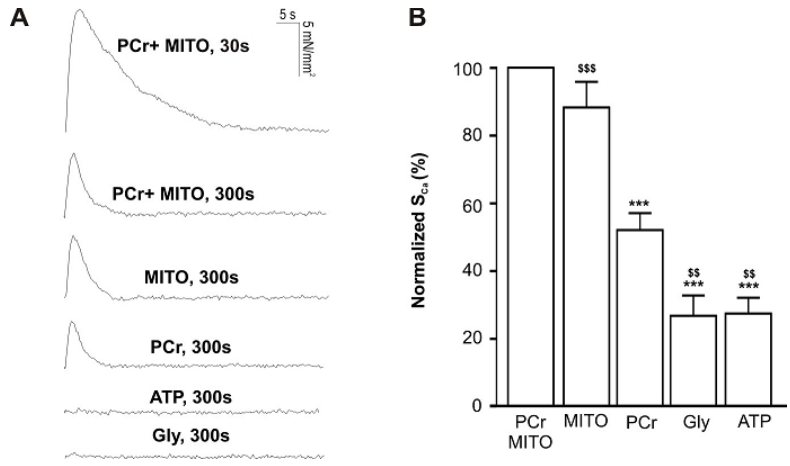

Figure 21. Different effects of various energetic conditions on SR Ca^{2+} loss via the Ca^{2+} pump. All solutions contained 3.16 mM MgATP. Energetic conditions were: 12 mM PCr and activated mitochondria (PCr + MITO; optimal conditions); 12 mM PCr and inhibited mitochondria (PCr); activated mitochondria (MITO); glycolytic intermediates and NAD (Gly); ATP alone (ATP). (A) Force transients elicited by 5 mM caffeine after 5 minutes of SR Ca^{2+} loading under optimal energetic conditions followed by 30 or 300 s incubation in *leak solution* under various energetic conditions. (B) Calculated $[Ca^{2+}]$-time integrals after 300 s incubation in *leak solution* under various energetic conditions normalized to corresponding values obtained under optimal energetic conditions (PCr+MITO). *** $p<0.001$ (n = 12–23) vs optimal energetic conditions taken as 100%. $$ $p<0.01$, $$$ $p<0.001$ vs PCr.

DISCUSSION

1. Cation fluxes to the mitochondria induce mitochondrial swelling and affect cellular functions

Mitochondrial volume homeostasis is a housekeeping cellular function essential for maintaining the structural integrity of the organelle. Changes in mitochondrial volume have been associated with a wide range of important biological functions and pathologies. Mitochondrial matrix volume is controlled by the osmotic balance between the cytosol and mitochondria. Any imbalance in the fluxes of the main intracellular ion, potassium, will thus affect the osmotic balance between cytosol and the matrix and promote water movement between these two compartments (Kaasik *et al*., 2007). Here, we concentrated on the potential effects of mitochondrial swelling on the functioning of two different types of excitable cells, neurons and cardiomyocytes. The organization and the dynamics of mitochondria in these cell types are very different. In neurons, the mitochondria are highly motile, moving from the neuronal body to the periphery and back through relatively tiny axonal shafts (Chada and Hollenbeck, 2003; Nekrasova *et al*., 2007; Reis *et al*., 2009; Yi *et al*., 2004). The opposite situation is found in cardiomyocytes, where stationary mitochondria are tightly packed and occupy a significant part of the intracellular volume. Here, we demonstrated that in both cases mitochondrial swelling could induce mechanical interactions with neighbouring structures and affect the cell function.

1.1. Mitochondrial swelling impaires organelle trafficking in neurons

The length, complexity, and slenderness of neuronal processes coupled with the amount of material that must be transported makes axonal transport vulnerable to any kind of perturbation. Therefore, traffic jams are thought to be involved in the pathogenesis of several neurodegenerative diseases. Indeed, abnormalities in axonal transport have been demonstrated in models of amyotrophic lateral sclerosis (Collard *et al*., 1995; Munoz *et al*., 1988; Rouleau *et al*., 1996; Williamson and Cleveland, 1999; Zhang *et al*., 1997), several models of polyglutamine disease (Katsuno *et al*., 2006) as well as in paraplegia and drug-induced neuropathies (Ferreirinha *et al*., 2004).

We propose that size and morphology of the transported cargo are also relevant for seamless axonal transport, and we speculate that mitochondrial swelling could be one of the reasons for impaired organelle transport in neuronal processes. Current data demonstrate that mitochondrial swellers increasing the diameter and volume of mitochondria inhibit mitochondrial as

well as lysosomal traffic; all conditions leading to the inhibition of organelle transport in processes also lead to a parallel increase in mitochondrial diameter. In all cases, mitochondrial diameter increased from around 200 to 400–600 nm, which is larger than the average diameter of processes, which is around 200–300 nm. We clearly demonstrated that this inhibition is not related to the cessation of mitochondrial ATP production as proposed earlier (Miller and Sheetz, 2006; Rintoul *et al*., 2003; Safiulina *et al*., 2006); bongkrekic acid and oligomycin, which inhibit ATP transport from the mitochondrial matrix to the cytosol and mitochondrial ATP synthetase, respectively, had no effect on mitochondrial or lysosomal traffic. The absence of their effect could be explained by earlier data demonstrating that glycolysis can support the function of cerebellar granule cells *in vitro* (Budd and Nicholls, 1996), and by the observations that molecular motors responsible for mitochondrial traffic have a relatively high affinity to ATP (Hollenbeck, 1996). It is also unlikely that mitochondrial depolarization *per se* induced by swellers could affect axonal traffic. The mitochondrial membrane potential could modify mitochondrial binding to the motor proteins or motor protein activity, but not lysosomal traffic directly. It is therefore most tempting to speculate that swollen mitochondria physically block the passage of other sized organelles in neurites, and thus, inhibit axonal organelle traffic. Several observations support this hypothesis; swollen mitochondria tend to block mitochondrial movement, and this interaction seemed to be less evident in larger neurites.

1.2. Mitochondrial swelling increases passive force and leads to nuclear compression in cardiomyocytes

This study is the first to demonstrate that densely packed cells such as cardiomyocytes are able to rapidly generate an internal pressure which can mechanically affect morphological as well as functional properties of intracellular organelles. The study of mechano-transduction has historically focused on how externally applied forces can affect cell signalling and function. However, a growing body of evidence suggests that the forces generated internally are as important in regulating cell behaviour (Wozniak and Chen, 2009). Here, we identify a novel source of intracellular force: the mitochondria.

Using nuclear volume and passive tension as intracellular force sensors, we have been able to show that dramatic intracellular forces are generated by swollen mitochondria in cardiomyocytes. Given the tight packing of organelles and myofibrils in cardiomyocytes, the significant volume occupied by mitochondria (32–45%) of cell volume in adult mouse cardiomyocytes), and the extremely low free cytosolic volume (around 4–7% of the cell volume), any increase in mitochondrial mass will automatically be at the expense of the volume of other compartments (Ventura-Clapier *et al*., 2008 and references therein). The physical constraints of cardiomyocytes also make large increases in the volume of subcellular structures impossible.

The myofilaments and nuclei are perhaps the most likely structures to respond to increased intracellular pressure. Indeed, the myofibrillar compartment is known to be rather compressible. Osmotic compression, for example, caused by a weak increase in 500 kDa dextran concentration, decreases the cardiac myofibrillar lattice spacing by about 20% (Farman *et al*., 2006).

The distance between thick and thin filaments is suggested to be an important determinant of active and passive tension. As myosin and actin filaments come closer together, both myofilament Ca^{2+} sensitivity (Farman *et al*., 2006; Harrison *et al*., 1988; Wang and Fuchs , 1995) and maximal Ca^{2+}-induced tension (Fukuda *et al*., 2001) increase. This could be explained by the hypothesis that the number of strong-binding cross-bridges that are formed is directly related to the proximity of myosin heads to the binding sites on actin (Yagi *et al*., 2004). However, compression of the myofibrillar compartment is also able to increase a calcium-independent force rigor tension (Kaasik *et al*., 2004), as well as passive tension (Martyn *et al*., 2004; Roos and Brady, 1990). In addition, the distance between protein filaments can affect the probability of weak cross-bridges forming, thus modulating the passive characteristics of cardiac muscle (Martyn *et al*., 2004) and titin-based passive force (Cazorla *et al*., 2001). In summary, compression of the myofibrillar compartment might be a factor that modulates both the contractility and passive characteristics of the myocardium. Our results suggest that increases in mitochondrial volume could induce a marked reduction in lattice spacing and a concomitant increase in passive force.

One may speculate that the mechanism we describe could link mitochondrial swelling to the increased passive force observed in an ischaemic myocardium. The contractile properties of myofibrils are very sensitive to rapid metabolic changes occurring in the cytosol, such as changes in pH and the concentration of inorganic phosphate and adenine nucleotides. For example, in ischaemia such metabolic changes inhibit active force generation and elevate passive force and myocardial stiffness. Also, mitochondrial volume, which is regulated by an electrochemical potential-sensitive ionic flux across the inner mitochondrial membrane, seems to be increased under ischaemic conditions. As a consequence, swollen mitochondria may compress the neighbouring myofilaments, thus increasing both passive force/stiffness and active force in the ischaemic myocardium without increasing energy expenditure. This could be an important adaptive mechanism under conditions in which the contractile force is depressed due to the cytosolic accumulation of protons and inorganic phosphate. Alternative explanation for increase in passive stiffness during ischaemia could be related with energy deficiency and formation of rigor tension.

In the present work, we also showed that mitochondria are able to mechanically compress the nucleus and to change its geometry. Such an effect is not trivial, because the nucleus is the stiffest cell organelle (Caille *et al*., 2002; Dahl *et al*., 2008). It is therefore surprising that mitochondrial swelling induced by alamethicin and propranolol leads to a drastic modification of

nuclear shape. The mitochondria were able to completely change the usual, oval geometry of the nuclei, thus revealing the existence of a great potential force arising from the interior of the cell.

Although we saw significant nuclear deformation when mitochondria were considerably swollen, even with the moderate swelling induced by valinomycin and diazoxide, which was difficult to visualize using confocal microscopy, nuclear compression was observed. Since the volume of the nuclear envelope was not augmented, it can be concluded that the volume of the nuclear interior of the nucleus was reduced as a result of mitochondrial swelling.

A question of great importance is how the modulation of nuclear shape by mechanical signalling influences cell function. For many mechano-transduction events, the downstream cellular pathways of force-sensed gene transcription are well characterized (for a review, see Dahl *et al*., 2008). Various mechanisms have been proposed to explain how the forces that affect nuclear shape modulate gene transcription. Inside the nucleus, such forces could result in conformational changes to the DNA double helix or the higher-order chromatin structure, which could then lead to changes in transcriptional activity. Force can induce remodelling and disassembly of the macromolecules, thus influencing transcriptional processes (for a review, see Zlatanova and Leuba, 2002; Marko and Poirier, 2003). In addition to the direct effects of force on DNA structure, nuclear deformation could also result in the large-scale reorganization of genes within the nucleus (Dahl *et al*., 2008). Mechanical stress may also have an impact on nuclear transport processes since it has been shown that nuclear pore complexes function in a mechanically sensitive manner (Wolf and Mofrad, 2008).

In this work we have demonstrated that diazoxide, an opener of mitochondrial K_{ATP} channels, induces significant compression of nuclei. It is well known that diazoxide exerts a cardioprotective action by mimicking the infarct size-limiting effect of preconditioning, i.e. by increasing the resistance to ischaemia. Such resistance needs time to be developed after diazoxide administration, and it is abolished by 5-HD, a putative blocker of K_{ATP} channels (for a review, see O'Rourke, 2004). The mechanism of the post-ischaemic protection induced by diazoxide remains unclear, but most hypotheses propose that modulation of mitochondria via K_{ATP} channel opening is a triggering signal. Interestingly, various drugs inducing mitochondrial matrix swelling elicit cardioprotection (Juhaszova *et al*., 2004; O'Rourke, 2004). It is tempting to speculate that nuclear compression caused by diazoxide-induced mitochondrial swelling might somehow modulate nuclear function, involving the activation of cellular cascade(s) that lead to increased cardiac resistance to ischaemic stress. This speculation is supported by our observation that 5-HD, which usually antagonizes the protective effect of diazoxide, is able to completely abolish diazoxide-induced nuclear compression.

It is possible that changes in mitochondrial geometry within cardiomyocytes influence not only the myofibrils and nuclei but also other organelles. As an

example, mechanical signals may displace the internal junctions between the SR and T-tubules which are responsible for functional interactions between dihydropyridine and ryanodine receptors, or they may displace the structural contacts between the SR and mitochondria which are involved in the control of Ca^{2+} homeostasis, excitation–contraction coupling, and the regulation of adenine nucleotide channelling.

In conclusion, we have shown that in the cardiomyocyte *in situ*, mitochondria represent a source of significant internal force production. The force they can exert is able to compress both myofibrillar and nuclear compartments. This suggests a potential role for mitochondrial swelling in the regulation of myofilament and nuclear functions by internal mechanical signalling.

2. ER calcium fluxes are modulated by monovalent cations and cellular energetic state

2.1. ER potassium fluxes control ER calcium uptake

Our work is the first to demonstrate that KHE and SK_{Ca} reside in the ER membrane and that their activity is a perquisite for ER Ca^{2+} uptake.

The KHE was previously earlier found on the inner mitochondrial membrane where it allows intramitochondrial potassium to exchange with extramitochondrial protons. It has been shown that this is essential for controlling mitochondrial volume and that its inhibition leads to extreme mitochondrial swelling (Dimmer *et al* 2008; Kaasik *et al*., 2004; Nowikovsky *et al*., 2004; Safiulina *et al*., 2006). KHE is coded by the *LETM1* gene and is considered to reside only in the mitochondrial inner membrane (Froschauer *et al*., 2005; McQuibban *et al*., 2010; Nowikovsky *et al*., 2004). However, in addition to its N-terminal mitochondrial targeting sequence, LETM1 has the ER membrane retention signal AEVK in its C-terminus. Indeed, our immunohistochemical experiments with the LETM1-specific antibody demonstrated its colocalization with the ER in neurons, and a clear ER resembling localization in cardiomyocytes. Moreover, high LETM1 levels were detected from the purified ER fraction.

Our results also demonstrated that ER KHE activity is required for ER Ca^{2+} uptake. Inhibition of the KHE exchanger in permeabilized neurons or cardiac fibres by propranolol or quinine completely inhibited ER Ca^{2+} uptake.

What could be the physiological relevance of KHE of ER membrane? The SERCA acts as an antiporter: for every two Ca^{2+} ions pumped to the ER two to three protons from the ER lumen are released into the cytoplasm (Levy *et al*., 1990). In addition, the influx of chloride counter-ions through CIC chloride channels will lead to proton extrusion from the ER lumen (Jentsch, 2007; Picollo and Pusch, 2005; Plans *et al*., 2009; Scheel *et al*., 2005). Without proton re-entry into the ER lumen this would alkalize the ER lumen and block SERCA

activity (Peinelt and Apell, 2002). Our experiments strongly suggest that protons could re-enter the ER lumen through the KHE.

Our second finding is that SK_{Ca} channels are localized in the ER membrane and participate in ER Ca^{2+} uptake. The SK_{Ca} channel subfamily contains four members - SK1-4 (or KCNN1-4) (Joiner *et al*., 1997). Although they were only found in the plasma membrane (Dai *et al*., 2009; Maylie *et al*., 2004), some of SK_{Ca} channels proteins have ER membrane retention signals in their N-terminus that could target them to ER membrane. However, to the best of our knowledge, there is currently no data concerning their intracellular localization and our report is the first to demonstrate this. Using an antibody recognizing the SK1-3 channels, we showed that SK_{Ca} channels colocalize with the ER marker in neurons and that their localization resembles the SR membrane in cardiomyocytes.

In the plasma membrane, activation of SK_{Ca} channels by a rise in intracellular Ca^{2+} favours the outward K^+ current and hyperpolarization of the membrane. Therefore, it could be presumed that a rise in intracellular Ca^{2+} will also activate ER SK_{Ca} channels and the K^+ current from the cytoplasm to the ER lumen. It also seems that these K^+ fluxes are relevant for ER Ca^{2+} uptake. Our results demonstrate that two selective non-peptidic SK_{Ca} channel blockers, dequalinium and UCL 1684, partially inhibit ER Ca^{2+} uptake in neurons and completely inhibit this in cardiac fibres. This suggests that SK_{Ca} channels serve as a route for K^+ re-entry during Ca^{2+} uptake. During the uptake phase, KHE exports K^+ and the ER may need a mechanism to restore potassium homeostasis across the ER membrane. Our data suggests that SK_{Ca} channels may serve as one possible mechanism for potassium re-entry. It is noteworthy that this channel is under the control of cytoplasmic Ca^{2+}. We can thus speculate that high cytoplasmic Ca^{2+} levels could favour opening of the ER SK_{Ca} channels in a similar manner to plasma membrane SK_{Ca} channels which will facilitate KHE function, proton re-entry and thus SERCA activity. However, the fact, that SK_{Ca} channels could also be used for potassium efflux from the ER cannot be excluded. The counter-transport of protons by the SERCA could not fully ensure the charge balance and a further efflux of positive ions or an influx of negative ions is required for complete charge equilibrium.

Our discovery may also contribute to the understanding of WFS. Wolf-Hirschhorn Syndrome is a complex congenital syndrome caused by a monoallelic deletion of the short arm of chromosome 4 (Endele *et al*., 1999). The variation and severity of the symptoms in WHS patients is linked to the size of the chromosome deletion and it is now widely recognized that the various symptoms cannot result from the loss of a single pathogenic gene. The *LETM1* gene has been identified as an excellent candidate gene for causing seizures in WHS (South *et al*., 2007; Zollino *et al*., 2003). To date, these effects have been mostly associated with deficient mitochondrial KHE and mitochondrial osmoregulation (McQuibban *et al*., 2010). However, our results demonstrating the participation of ER LETM1 in intracellular Ca^{2+} cycling allow to suggest that deficient ER Ca^{2+} handling might also be involved.

In summary, our work demonstrates that the ER membrane contains KHE and SK_{Ca} channels which are involved in ER Ca^{2+} uptake (see also the proposed model in Fig. 22).

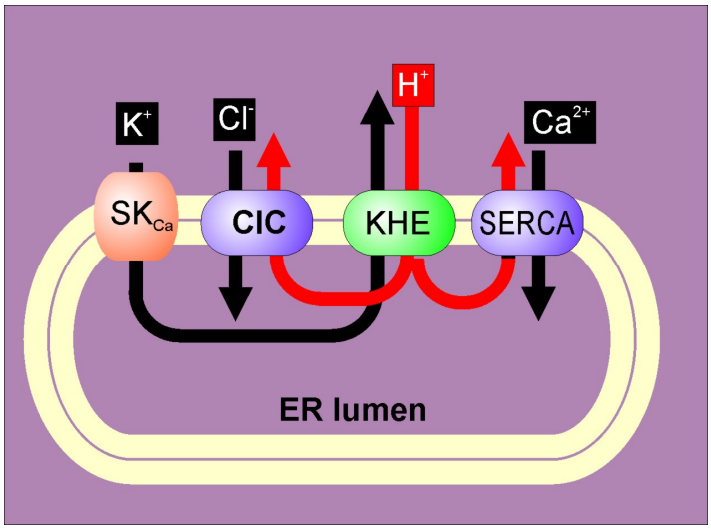

Figure 22. Proposed model of counter-ion movement through the ER membrane during Ca^{2+} uptake. Ca^{2+} ions are pumped to the ER by SERCA. This is accompanied by the counter-transport of protons (two to three protons for every two Ca^{2+} ions). To compensate the remaining positive charge, Cl^- ions enter through CIC channels, accompanied again by the extrusion of protons (one proton per two Cl^- ions). To avoid matrix alkalization and concomitant inhibition of SERCA, protons re-entry through the KHE (or LETM1). To compensate for the loss of K^+ ions from the SR lumen, K^+ may re-enter through the SK_{Ca} channels which are open only during the uptake phase.

2.2. Energetic state regulates SR calcium loss in cardiac muscle

The amount of releasable Ca^{2+} in the SR depends not only on the Ca^{2+} uptake rate but also on Ca^{2+} loss during the resting period. The results obtained in the present study were: (I) *in situ*, in the absence of extra-reticular Ca^{2+}, this ion rapidly leaks out of the SR compartment; (II) this leak mainly occurs by a backward flux through the SERCA; (III) the leak strongly depends on the cellular energy state; (IV) direct energy cross-talk between mitochondria and SERCA is more efficient at inhibiting the SR Ca^{2+} leak than the local ADP re-phosphorylation catalysed by bound CK; (V) the leak at physiological diastolic $[Ca^{2+}]$ is also energy-dependent.

Our results confirm that, at least under conditions of a high intra/extra-reticular Ca^{2+} gradient, the SR *in situ* is rather 'leaky' in that intra-reticular Ca^{2+} levels start to rapidly decrease if cytosolic $[Ca^{2+}]$ drops. The decrease in the SR Ca^{2+} content in a Ca^{2+}-free medium, as visualized by fluorescent dye, is

concomitant with a reduction in the amount of releasable Ca^{2+} by the SR. The amount of this 'physiologically active' Ca^{2+}, which is able to activate myofibrils, was estimated from tension transients elicited by a caffeine-induced Ca^{2+} release.

An important question is what the main route of this Ca^{2+} leak is from the SR is under conditions of a high intra/extra-reticular Ca^{2+} gradient. In addressing this question, we inhibited SERCA during the leak period to decrease the reverse Ca^{2+} flux via this pump. SERCA inhibition caused a considerable increase in the amount of releasable SR Ca^{2+}. This increase could not have resulted from the unspecific effects of CPA or TBQ on RyR because these inhibitors do not reduce RyR-mediated Ca^{2+} leak (Dettbarn and Palade, 1998). Thus, these data indicate that the SR Ca^{2+} pump is directly involved in the Ca^{2+} leak under our experimental conditions.

In contrast to the effects of SERCA inhibition, the RyR antagonists did not reduce SR Ca^{2+} loss. Neither tetracaine nor RR was able to increase the amount of releasable Ca^{2+} under the conditions of a high Ca^{2+} leak. Some studies (Gyorke *et al*., 1997; Overend *et al*., 1998) whivh were performed using intact cardiac cells showed that significant diastolic Ca^{2+} leak occurs via the RyR, especially in cardiac pathology (Lehnart *et al*., 2006; Marks *et al*., 2002; Marks, 2003). However, several other studies support our findings. In voltage-clamped cardiac myocytes, for example, reverse flux through the SR Ca^{2+} pump was found to be the main pathway of diastolic Ca^{2+} flux from the SR (Shannon *et al*., 2000). Similarly, using isolated cardiac SR vesicles, Shannon *et al*. (2001) showed that at low external [Ca^{2+}] (100 nM), the passive leak via the RyR is extremely low relative to backward flux through the Ca^{2+} pump. The reverse mode of the Ca^{2+} pump was also found to be the main contributor to passive leak in SR vesicles isolated from skeletal muscle (Du *et al*., 1996). The relevance of these data should of course be considered, given that under physiological conditions diastolic [Ca^{2+}] is ~100 nM rather than zero. Such a physiological concentration would decrease the intra/extra-reticular gradient and thereby inhibit Ca^{2+} loss. Indeed, at 100 nM Ca^{2+} and under optimal energetic conditions, the SR Ca^{2+} content was almost the same after 30 or 300 s of leak period. However, in the presence of ATP only, the backward Ca^{2+} flux significantly decreased the amount of releasable Ca^{2+}. A rough estimation shows that poor energetic conditions during 5 min of incubation could be responsible for the loss of ≈50% of the Ca^{2+} pumped in a period of the same duration. Interestingly, inhibition of the potentially active RyR pathway by tetracaine did not significantly reduce Ca^{2+} loss. Thus, it can be concluded that energetic disturbances are able to activate a backward Ca^{2+} flux in living cells in diastole.

When analysing the mechanism of an energy-dependent Ca^{2+} loss, it is important to realize that the driving force for the Ca^{2+} flux is not only determined by the kinetic parameters of high energy phosphates but also by the thermodynamic equilibrium between the substrate and the products of ATPase

reaction. This reaction coupled to the translocation of two Ca^{2+} for each ATP is fully reversible. The reversal condition depends on the relationship between the free energy of ATP hydrolysis and the energy required to transport Ca^{2+} against the concentration gradient. The SERCA pump will cycle in the forward direction when the free energy of ATP hydrolysis (which depends on the ratio of MgATP to its hydrolysis products) is higher than the energy of the Ca^{2+} concentration gradient (Tran *et al*., 2009). When ADP and/or inorganic phosphate accumulate, the free energy of ATP hydrolysis drops and the pump will stop or even cycle in the reverse direction. Therefore, elimination of the products of ATP hydrolysis in the vicinity of SERCA is a prerequisite for preventing SR Ca^{2+} uptake inhibition (or preventing the SR Ca^{2+} loss coupled to ATP synthesis). Of course, specific assessments of such a reversibility of the Ca^{2+} pump needs more data concerning the actual magnitude of the phosphorylation potential near the SERCA and the intra/extra-reticular Ca^{2+} gradient.

The most interesting result of the present work is the finding of a differential sensitivity of the backward Ca^{2+} flux to various energy sources *in situ*. This flux is markedly decreased in the presence of various functioning systems able to locally re-phosphorylate ADP. Importantly, there are differences in the relative efficiency of these various systems. Our results show that the regeneration of ATP by endogenous glycolytic enzymes had a negligible effect on the reverse mode of the Ca^{2+} pump. This result was unexpected, because in the same model glycolytic support strongly increased Ca^{2+} loading (Boehm *et al*., 2000). Therefore, it is possible that glycolytic enzyme activation needs a certain Ca^{2+} concentration. Stimulation of the endogenous CK system caused considerable inhibition of Ca^{2+} loss; however, direct adenine nucleotide channelling mediated by cross-talk between the mitochondria and SERCA was even more efficient in inhibiting the backward Ca^{2+} flux from the SR.

Interestingly, the efficacy of CK and mitochondria in supporting SR Ca^{2+} pumping is quite similar (Kaasik *et al*., 2001). Higher efficacy of mitochondria in blocking the reverse mode of the SR Ca^{2+} pump found in the present work enables us to hypothesize that energetic regulation of the forward and backward flux is not identical. Of possible relevance to such a hypothesis is the activation of backward flux by inorganic phosphate (Winkler *et al*., 1977; Smith *et al*., 2000). In fact, local ATP regeneration by mitochondria is coupled to equimolar inorganic phosphate (Pi) consumption, such that phosphate produced locally by the SERCA is completely eliminated. In contrast, ATP regeneration by the CK system does not involve Pi consumption, so that high ATPase activity even in the presence of effective ATP regeneration at the expense of PCr could create an increased Pi concentration in the vicinity of the SR compartment. This, in turn, would favour the backward Ca^{2+} flux, which could explain the lower efficacy of the CK system in inhibiting Ca^{2+} loss from the SR.

The increased backward Ca^{2+} flux due to perturbations in the SERCA energy supply could contribute to decreased cardiac contractility in pathological conditions, especially heart failure. The failing heart is characterized by

multiple alterations in energy metabolism (for a review, see Ventura-Clapier *et al*., 2004). Furthermore, the ultrastructure of failing cardiac cells is profoundly disorganized (see Hein *et al*., 2000, 2001 and references therein), such that structural relationships between cell compartments are altered. This should affect cross-talks between organelles, including those involved with energetics. Consistent with this, we have previously shown (Wilding *et al*., 2006) that cell remodelling induced by the muscle LIM protein-null mutation caused a decrease in the mitochondrial support for SR Ca^{2+} uptake, despite unchanged mitochondrial content and a normal intrinsic mitochondrial function. Thus, direct energy channelling between mitochondria and SERCA, being the main energetic factor inhibiting the reverse mode of the SERCA, seems to be a mechanism which could be easily altered in heart failure due to cell remodelling (Joubert *et al*., 2008).

Altogether, our results have shown (Fig. 23) that at a low extra-reticular Ca^{2+}, the backward SR flux strongly depends on the cell energy state and the main inhibitor of this Ca^{2+} loss is energy channelling between the mitochondria and SERCA rather than CK-catalysed energy support. This suggests that functional uncoupling between the mitochondria and SERCA due to cell remodelling in cardiac pathologies could impair function of the SR via increased SR Ca^{2+} loss.

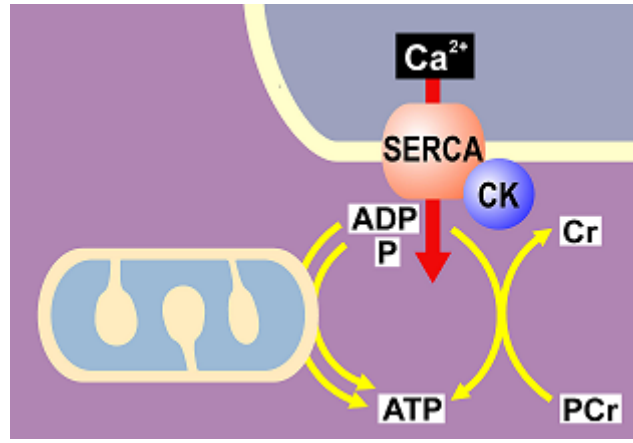

Figure 23. Energetic regulation of backward Ca^{2+} flux inhibition. The sarcoplasmic reticulum Ca^{2+} pump is able to mediate a significant backward flux. This flux strongly depends on the local ATP/ADP ratio in the vicinity of SERCA and may be inhibited by two energetic pathways. The first one is mediated by CK bound to SR; the second one is mediated by direct adenine nucleotide channelling between SERCA and juxtaposed mitochondria. Mitochondria seem to be more efficient than CK in inhibiting the flux, probably due to their ability to decrease the local inorganic phosphate concentration. Cardiac pathologies, which induce CK down-regulation and/or dissociation between mitochondria and SR due to cell remodelling, could favour the SERCA-mediated Ca^{2+} backward flux and compromise contractility.

CONCLUSIONS

Monovalent cation fluxes across intracellular membranes in neurons and cardiomyocytes play important roles in the cell functioning. They are involved in intracellular signalling, organelle trafficking and calcium homeostasis. Here we demonstrated that:

1) Swollen mitochondria can impair organelle transport in neurons by physically blocking the passage of other sized organelles in neurites independently, and thus can inhibit the axonal organelle traffic.

2) Swollen mitochondria can generate intracellular forces that are able to compress myofilaments as well as nucleus in cardiomyocytes. This suggests that mitochondria represent a source of significant internal force production that has potential role in internal mechanical signalling.

3) The ER proton and potassium fluxes through the KHE and SK_{Ca} channels play major role in ER Ca^{2+} uptake both in neurons and in cardiomyocytes.

4) Cellular energetic state regulates SR Ca^{2+} loss through the SERCA in cardiac muscle. Direct energy channelling from the mitochondria is the most effective energy pathway, which is also able to inhibit the SERCA-dependent Ca^{2+} leak.

REFERENCES

Abramcheck CW, Best PM. Physiological role and selectivity of the *in situ* potassium channel of the sarcoplasmic reticulum in skinned frog skeletal muscle fibers. *J Gen Physiol* 1989;93:1–21.

Alberts B, Johnson A, Lewis J, Raff M, Roberts K, Walter P. Molecular biology of the cell. 4th edition. Garland Science, New York. 2002; Ch 17:555–558.

Ardail D, Gasnier F, Lermé F, Simonot C, Louisot P, Gateau-Roesch O. Involvment of mitochondrial contact sites in the subcellular compartmentalization of phospholipid biosynthetic enzymes. *J Biol Chem* 1993;268:25985–25992.

Arnaudeau S, Kelley WL, Walsh JV Jr, Demaurex N. Mitochondria recycle Ca2+ to the endoplasmic reticulum and prevent the depletion of neighboring endoplasmic reticulum regions. *J Biol Chem* 2001;276:29430–29439.

Bechinger B. Structure and functions of channel-forming peptides: magainins, cecrophins, melittin and alamethicin. *J Membr Biol* 1997;156:197–211.

Bednarczyk P. Potassium channels in brain mitochondria. Acta Biochim Pol 2009;56:385–392.

Benquet P, Le Guen J, Pichon Y, Tiaho F. Differential involvement of Ca(2+) channels in survival and neurite outgrowth of cultured embryonic cockroach brain neurons. *J Neurophysiol* 2002; 88:1475–1490.

Bernardi P. Mitochondrial transport of cations: channels, exchangers, and permeability transition. *Physiol Rev* 1999;79:1127–1155.

Berridge MJ. The endoplasmic reticulum: a multifunctional signaling organelle. *Cell Calcium* 2002;32:235–249.

Bers DM, Barry WH, Despa S. Intracellular Na+ regulation in cardiac myocytes. *Cardiovasc Res* 2003;57:897–912.

Bers DM, Eisner DA, Valdivia HH. Sarcoplasmic reticulum Ca2+ and heart failure: roles of diastolic leak and Ca2+ transport. *Circ Res* 2003;93:487–490.

Boehm E, Ventura-Clapier R, Mateo P, Lechene P, Veksler V. Glycolysis supports calcium uptake by the sarcoplasmic reticulum in skinned ventricular fibres of mice deficient in mitochondrial and cytosolic creatine kinase. *J Mol Cell Cardiol* 2000;32:891–902.

Bowler MW, Montgomery GM, Leslie AG, Walker JE. How azide inhibits ATP hydrolysis by the F-ATPases. *Proc Natl Acad Sci U S A* 2006;103:8646–8649.

Brookes PS, Yoon Y, Robotham JL, Anders MW, Sheu SS. Calcium, ATP, and ROS: a mitochondrial love-hate triangle. *Am J Physiol Cell Physiol* 2004;287:817–833.

Budd SL, Nicholls DG. Mitochondria, calcium regulation, and acute glutamate excitotozicity in cultured cerebellar granule cells. *J Neurochem* 1996;67:2282–2291.

Caille N, Thoumine O, Tardy Y, Meister JJ. Contribution of the nucleus to the mechanical properties of endothelial cells. *J Biomech* 2002;35:177–187.

Cammann K, Ion-selective bulk membranes as models, *Top. Curr. Chem* 1985; 128:219–258.

Cazorla O, Wu Y, Irving TC, Granzier H. Titin-based modulation of calcium sensitivity of active tension in mouse skinned cardiac myocytes. *Circ Res* 2001;88:1028–1035.

Chada SR, Hollenbeck PJ. Mitochondrial movement and positioning in axons: the role of growth factor signaling. *J Exp Biol* 2003;206:1985–1992.

Chen H, Chan DC. Critical dependence of neurons on mitochondrial dynamics. *Curr Opin Cell Biol* 2006;18:453–459.

Colegrove SL, Albrecht MA, Friel DD. Dissection of mitochondrial Ca2+ uptake and release fluxes *in situ* after depolarization-evoked [Ca2+]i elevations in sympathetic neurons. *J Gen Physiol* 2000;115:351–370.

Collard JF, Côté F, Julien JP. Defective axonal transport in a transgenic mouse model of amyotrophic lateral sclerosis. *Nature* 1995;375:61–64.

Cortassa S, Aon MA, Marbán E, Winslow RL, O'Rourke B. An integrated model of cardiac mitochondrial energy metabolism and calcium dynamics. *Biophys J* 2003;84:2734–55.

Csordas G, Renken C, Varnai P, Walter L, Weaver D, Buttle KF, Balla T, Mannella CA, Hajnoczky G. Structural and functional features and significance of the physical linkage between ER and mitochondria. *J Cell Biol* 2006;174:915–921.

Dahl KN, Ribeiro AJ, Lammerding J. Nuclear shape, mechanics, and mechano-transduction. *Circ Res* 2008;102:1307–1318.

Dai S, Hall DD, Hell JW. Supramolecular assemblies and localized regulation of voltage-gated ion channels. *Physiol Rev* 2009;89:411–52.

Dairaku N, Kato K, Honda K, Koike T, Iijima K, Imatani A, Sekine H, Ohara S, Matsui H, Shimosegawa T. Oligomycin and antimycin A prevent nitric oxide-induced apoptosis by blocking cytochrome C leakage. *J Lab Clin Med* 2004; 143: 143–151.

Dash RK, Beard DA. Analysis of cardiac mitochondrial Na+-Ca2+ exchanger kinetics with a biophysical model of mitochondrial Ca2+ handing suggests a 3:1 stoichometry. *J Physiol* 2008;586:3267–3285.

Dettbarn C, Palade P. Effects of three sarcoplasmic/endoplasmic reticulum Ca2+ pump inhibitors on release channels of intracellular stores. *J Pharmacol Exp Ther* 1998;285:739–745.

Dhalla NS, Saini-Chohan HK, Rodriguez-Leyva D, Elimban V, Dent MR, Tappia PS. Subcellular remodeling may induce cardiac dysfunction in congestive heart failure. *Cardiovasc Res* 2009;81:429–438.

Dimmer KS, Navoni F, Casarin A, Trevisson E, Endele S, Winterpacht A, Salviati L, Scorrano L. LETM1, deleted in Wolf-Hirschhorn syndrome is required for normal mitochondrial morphology and cellular viability. *Hum Mol Genet* 2008;17:201–214.

Du GG, Ashley CC, Lea TJ. Ca2+ effluxes from the sarcoplasmic reticulum vesicles of frog muscle: effects of cyclopiazonic acid and thapsigargin. Cell Calcium 1996;20:355–359.

Duchen MR. Mitochondria and Ca2+ in cell physiology and pathophysiology. *Cell Calcium* 2000;28:339–348.

Endele S, Fuhri M, Pak SJ, Zabel BU, Winterpacht A. LETM1, a novel gene encoding a putative EF-hand Ca2+-binding protein, flanks the Wolf-Hirschhorn syndrome (WHS) critical region and is deleted in most WHS patients. *Genomics* 1999;60:218–225.

Farman GP, Walker JS, de Tombe PP, Irving TC. Impact of osmotic compression on sarcomere structure and myofilament calcium sensitivity of isolated rat myocardium. *Am J Physiol Heart Circ Physiol* 2006;291:1847–1855.

Ferreirinha F, Quattrini A, Pirozzi M, Valsecchi V, Dina G, Broccoli V, Auricchio A, Piemonte F, Tozzi G, Gaeta L, Casari G, Ballabio A, Rugarli EI. Axonal degeneration in paraplegin-deficient mice is associated with abnormal mitochondria and impairment of axonal transport. *J Clin Invest* 2004;113:231–242.

Froschauer E, Nowikovsky K, Schweyen RJ. Electroneutral K+/H+ exchange in mitochondrial membrane vesicles involves Yol027/Letm1 proteins. *Biochim Biophys Acta* 2005;1711:41–48.

Fukuda N, O-Uchi J, Sasaki D, Kajiwara H, Ishiwata S, Kurihara S. Acidosis of inorganic phosphate enhances the length dependence of tension in rat skinned cardiac muscle. *J Physiol* 2001;536:153–160.

Garlid KD, Paucek P. Mitochondrial potassium transport: the K (+) cycle. *Biochim Biophys Acta* 2003;1606:23–41.

Gunter TE, Buntinas L, Sparagna G, Eliseev R, Gunter K. Mitochondrial calcium transport: mechanisms and functions. *Cell Calciuim* 2000;28:285–296.

Gunter TE, Pfeiffer DR. Mechanisms by which mitochondria transport calcium. *Am J Physiol* 1990;258:755–786.

Gustafsson AB, Gottlieb RA. Heart mitochondria: gates of life and death. *Cardiovasc Res* 2008;77:334–343.

Gyorke S, Lukyanenko V, Gyorke I. Dual effects of tetracaine on spontaneous calcium release in rat ventricular myocytes. *J Physiol* 1997;500:297–309.

Hajnoczky G, Czordas G, Madesh M, Pacher P. The machinery of local Ca2+ signalling between sarco-endoplasmic reticulum and mitochondria. *J Physiol* 2000;529:69–81.

Halestrap AP. The regulation of the matrix volume of mammalian mitodchondria in vivo and in vitro and its role in the control of mitochondrial metabolism. *Biochim Biophys Acta* 1989;973:355–382.

Harris DA, Das AM. Control of mitochondrial ATP synthesis in the heart. *Biochem J* 1991;280:561–573.

Harrison SM, Lamont C, Miller DJ. Hysteresis and the length dependence of calcium sensitivity in chemically skinned rat cardiac muscle. *J Physiol* 1988;401:115–143.

Hasenfuss G, Pieske B. Calcium cycling in congestive heart failure. *J Mol Cell Cardiol* 2002;34:951–969.

Hein S, Arnon E, Kostin S, Schonburg M, Elsasser A, Polyakova V, Bauer EP, Klovekorn WP, Schaper J. Progression from compensated hypertrophy to failure in the pressure-overloaded human heart: structural deterioration and compensatory mechanisms. *Circulation* 2003;107:984–991.

Hein S, Kostin S, Heling A, Maeno Y, Schaper J. The role of the cytoskeleton in heart failure. *Cardiovasc Res* 2000;45:273–278.

Henderson PJ, Lardy HA. Bongkrekic acid. An inhibitor of the adenine nucleotide translocase of mitochondria. *J Biol Chem* 1970;245:1319–1326.

Hollenbeck PJ, Saxton WM. The axonal transport of mitochondria. *J Cell Sci* 2005;118:5411–5419.

Hollenbeck PJ. The pattern and mechanism of mitochondrial transport in axons. Front Biosci 1996;1:91–102.

Jentsch TJ. Chloride and the endosomal-lysosomal pathway: emerging roles of CLC chloride transporters. *J Physiol* 2007;578:633–640.

Johnson VP, Mulder RD, Hosen R. The Wolf-Hirschhorn (4p-) syndrome. *Clin Genet* 1976;10:104–12.

Joiner WJ, Wang LY, Tang MD, Kaczmarek LK. hSK4, a member of a novel subfamily of calcium-activated potassium channels. *Proc Natl Acad Sci U S A* 1997;94:11013–11018.

Jouaville LS, Pinton P, Bastianutto, Rutter GA, Rizzuto R. Regulation of mitochondrial ATP synthesis by calcium: Evidence for a long-term metabolic priming. *Proc Natl Acad Sci U S A* 1999;96:13807–13812.

Joubert F, Wilding JR, Fortin D, Domergue-Dupont V, Novotova M, Ventura-Clapier R, Veksler V. Local energetic regulation of sarcoplasmic and myosin ATPase is differently impaired in rats with heart failure. *J Physiol* 2008; 586:5181–5192.

Juhaszova M, Zorov DB, Kim SH, Pepe S, Fu Q, Fishbein KW, Ziman BD, Wang S, Ytrehus K, Antos CL, Olson EN, Sollott SJ. Glycogen synthase kinase-3beta mediates convergence of protection signaling to inhibit the mitochondrial permeability transition pore. *J Clin Invest* 2004;113:1535–1549.

Kaasik A, Joubert F, Ventura-Clapier R, Veksler V. A novel mechanism of regulation of cardiac contractility by mitochondrial functional state. *FASEB J* 2004;18:1219–1227.

Kaasik A, Safiulina D, Zharkovsky A, Veksler V. Regulation of mitochondrial matrix volume. *Am J Physiol Cell Physiol* 2007;292:157–163.

Kaasik A, Veksler V, Boehm E, Novotova M, Minajeva A, Ventura-Clapier R. Energetic crosstalk between organelles: archidectural integration of energy production and utilization. *Circ Res* 2001;89:153–159.

Katsuno M, Adachi H, Minamiyama M, Waza M, Tokui K, Banno H, Suzuki K, Onoda Y, Tanaka F, Doyu M, Sobue G. Reversible disruption of dynactin 1-mediated retrograde axonal transport in polyglutamine-induced motor neuron degeneration. *J Neurosci* 2006;26:12106–12117.

Kockskämper J, Zima AV, Roderick HL, Pieske B, Blatter LA, Bootman MD. Emerging roles of inostiol 1,4,5-triphosphate signaling in cardiac myocytes. *J Mol Cell Cardiol* 2008;45:128–147.

Lebiedzinska M, Szabadkai G, Jones AW, Duszynski J, Wieckowski MR. Interactions between the endoplasmic reticulum, mitochondria, plasma membrane and other subcellular organelles. *Int J Biochem Cell Biol* 2009;41:1805–1816.

Lehnart SE, Terrenoire C, Reiken S, Wehrens XH, Song LS, Tillman EJ, Mancarella S, Coromilas J, Lederer WJ, Kass RS, Marks AR. Stabilization of cardiac ryanodine receptor prevents intracellular calcium leak and arrhythmias. *Proc Natl Acad Sci U S A* 2006;103:7906–7910.

Levy D, Seigneuret M, Bluzat A, Rigaud JL. Evidence for proton countertransport by the sarcoplasmic reticulum Ca2+-ATPase during calcium transport in reconstituted proteoliposomes with low ionic permeability. *J Biol Chem* 1990;265:19524–19534.

Liu QY, Strauss HC. Blockade of cardiac sarcoplasmic reticulum K+ channel by Ca2+: two-binding-site model of blockade. *Biophys J* 1991;60:198–203.

Marko JF, Poirier MG. Micromechanics of chromatin and chromosomes. *Biochem Cell Biol* 2003;81:209–220.

Marks AR, Reiken S, Marx SO. Progression of heart failure: is protein kinase a hyperphosphorylation of the ryanodine receptor a contributing factor? *Circulation* 2002;105:272–275.

Marks AR. A guide for the perplexed: towards an understanding of the molecular basis of heart failure. *Circulation* 2003;107:1456–1459.

Martyn DA, Adhikari BB, Regnier M, Gu J, Xu S, Yu LC. Response of equatorial x-ray reflections and stiffness to altered sarcomere length and myofilament lattice spacing in relaxed skinned cardiac muscle. *Biophys J* 2004;86:1002–1011.

Maylie J, Bond CT, Herson PS, Lee WS, Adelman JP. Small conductance Ca2+–activated K+ channels and calmodulin. *J Physiol* 2004; 554:255–261.

McQuibban AG, Joza N, Megighian A, scorzeto M, Zanini D, Reipert S, Richter C, Schweyen RJ, Nowikovsky K. A Drosophila mutant of LETM1, a candidate gene for seizures in Wolf-Hirschhorn syndrome. *Hum Mol Genet* 2010;19:987–1000.

Mellon PL, Windle JJ, Goldsmith PC, Padula CA, Roberts JL, Weiner RI. Immortalization of hypothalamic GnRH neurons by genetically targeted tumorigenesis. *Neuron* 1990;5:1–10.

Michels G, Khan IF, Endres-Becker J, Rottlaender D, Herzig S, Ruhparwar A, Wahlers T, Hoppe UC. Regulation of the human cardiac mitochondrial Ca2+ uptake by 2 different voltage-gated Ca2+ channels. *Circulation* 2009;119:2435–2443.

Miller KE, Sheetz MP. Direct evidence for coherent low velocity axonal transport of mitochondria. *J Cell Biol* 2006;173:373–381.

Minajeva A, Ventura-Clapier R, Veksler V. Ca2+ uptake by cardiac sarcoplasmic reticulum ATPase in situ strongly depends on bound creatine kinase. *Pflugers Arch* 1996;432,904–912.

Munoz DG, Greene C, Perl DP, Selkoe DJ. Accumulation of phosphorylated neurofilaments in anterior horn motoneurons of amyotrophic lateral sclerosis patients. *J Neuropathol Exp Neurol* 1988;47:9–18.

Nekrasova OE, Kulik AV, Minin AA. Protein Kinase C regulates motility of mitochondria. *Biologicheskie Membrany* 2007;24:126–131.

Nowikovsky K, Froschauer EM, Zsurka G, Samaj J, Reipert S, Kolisek M, Wiesenberger G, Schweyen RJ. The LETM1/YOL027 gene family encodes a factor of the mitochondrial K+ homeostasis with a potential role in the Wolf-Hirschhorn syndrome. *J Biol Chem* 2004;279:30307–30315.

Nowikovsky K, Reipert S, Devenish RJ, Schweyen RJ. Mdm38 protein depletion causes loss of mitochondrial K+/H+ exchange activity, osmotic swelling and mitophagy. *Cell Death Differ* 2007;14:1647–1656.

Nowikovsky K, Schweyen RJ, Bernardi P. Pathophysiology of mitochondrial volume homeostasis: potassium transport and permeability transition. *Biochim Biophys Acta* 2009;1787:345–350.

O'Rourke B. Evidence for mitochondrial K+ channels and their role in cardioprotection. *Circ Res* 2004;94:420–432.

Overend CL, O'Neill SC, Eisner DA. The effect of tetracaine on stimulated contractions, sarcoplasmic reticulum Ca2+ content and membrane current in isolated rat ventricular myocytes. *J Physiol* 1998;507:759–769.

Palade G. Intracellular aspects of the process of protein synthesis. *Science* 1975:189:347–358.

Peinelt C, Apell HJ. Kinetics of the Ca2+, H+, and Mg2+ interaction with the ion-binding sites of the SR Ca-ATPase. *Biophys J* 2002;82:170–181.

Picollo A, Pusch M. Chloride/proton antiporter activity of mammalian CLC proteins ClC-4 and ClC-5. *Nature* 2005;436:420–423.

Plans V, Rickheit G, Jentsch TJ. Physiological roles of CLC Cl(–)/H(+) exchangers in renal proximal tubules. *Pflugers Arch* 2009;458:23–37.

Reis K, Fransson A, Aspenström P. The Miro GTPases: at the heart of the mitochondrial transport machinery. *FEBS Lett* 2009;583:1391–1398.

Rintoul GL, Filiano AJ, Brocard JB, Kress GJ, Reynolds IJ. Glutamate decreases mitochondrial size and movement in primary forebrain neurons. *J Neurosci* 2003;23:7881–7888.

Rizzuto R, Pinton P, Carrington W, Fay FS, Fogarty KE, Lifshitz LM, Tuft RA, Pozzan T. Close contacts with the endoplasmic reticulum as determinants of mitochondrial Ca2+ responses. *Science* 1998;280:1736–1766.

Roos KP, Brady AJ. Osmotic compression and stiffness changes in relaxed skinned cardiac myocytes in PVP-40 and dextran T-500. *Biophys J* 1990;58:1273–1283.

Rouleau GA, Clark AW, Rooke K, Pramatarova A, Krizus A, Suchowersky O, Julien JP, Figlewicz D. SOD1 mutation is associated with accumulation of neurofilaments in amyotrophic lateral sclerosis. *Ann Neurol* 1996;39:128–131.

Safiulina D, Veksler V, Zharkovsky A, Kaasik A. Loss of mitochondrial membrane potential is associated with increase in mitochondrial volume: physiological role in neurons. *J Cell Physiol* 2006;206:347–353.

Saks VA, Kaambre T, Sikk P, Eimre M, Orlova E, Paju K, Piirsoo A, Appaix F, Kay L, Regitz-Zagrosek V, Fleck E, Seppet E. Intracellular energetic units in red muscle cells. *Biochem J* 2001;356:643–657.

Scheel O, Zdebik AA, Lourdel S, Jentsch TJ. Voltage-dependent electrogenic chloride/proton exchange by endosomal CLC proteins. *Nature* 2005;436:424–427.

Shannon TR, Chu G, Kranias EG, Bers DM. Phospholamban decreases the energetic efficiency of the sarcoplasmic reticulum Ca pump. *J Biol Chem* 2001;276:7195–7201.

Shannon TR, Ginsburg KS, Bers DM. Quantitative assessment of the SR Ca2+ leak-load relationship. *Circ Res* 2002;91:594–600.

Shannon TR, Ginsburg KS, Bers DM. Reverse mode of the sarcoplasmic reticulum calcium pump and load-dependent cytosolic calcium decline in voltage-clamped cardiac ventricular myocytes. *Biophys J* 2000;78:322–333.

Shepherd GM, Harris KM. Three-dimensional structure and composition of CA3→CA1 axons in rat hippocampal slices: implications for presynaptic connectivity and compartmentalization. *J Neurosci* 1998;18:8300–8310.

Sherer NM, Lehmann MJ, Jimenez-Soto LF, Ingmundson A, Horner SM, Cicchetti G, Allen PG, Pypaert M, Cunningham JM, Mothes W. Visualization of retroviral replication in living cells reveals budding into multivesicular bodies. *Traffic* 2003;4:785–801.

Shi P, Gal J, Kwinter DM, Liu X, Zhu H. Mitochondrial dysfunction in amyotrophic lateral sclerosis. *Biochim Biophys Acta* 2010:1802:45–51.

Sobie EA, Guatimosim S, Gomez-Viquez L, Song LS, Hartmann H, Jafri MS, Lederer WJ. The Ca2+ leak paradox and "rogue ryanodine receptors": SR Ca2+ efflux theory and practice. *Prog Biophys Mol Biol* 2006;90:172–185.

South ST, Bleyl SB, Carey JC. Two unique patients with novel microdeletions in 4p16.3 that exclude the WHS critical regions: implications for critical region designation. *Am J Med Genet A* 2007;143:2137–2142.

Su B, Wang X, Zheng L, Perry G, Smith MA, Zhu X. Abnormal mitochondrial dynamics and neurodegenerative diseases. *Biochim Biophys Acta* 2010;1802:135–142.

Szewczyk A, Skalska J, Glab M, Kulawiak B, Malinska D, Koszela-Piotrowska I, Kunz WS. Mitochondrial potassium channels: from pharmacology to function. *Biochim Biophys Acta* 2006;1757:715–720.

Territo PR, French SA, Balaban RS. Simulation of cardiac work transitions, in vitro: effects of simultaneous Ca2+ and ATPase additions on isolated porcine heart mitochondria. Cell *Calcium* 2001;30:19–27.

Territo PR, Mootha VK, French SA, Balaban RS. Ca(2+) activation of heart mitochondrial oxidative phosphorylation: role of the F(0)/F(1)-ATPase. *Am J Phusiol Cell Physiol* 2000;278:423–435.

Tran K, Smith NP, Loiselle DS, Crampin EJ. A thermodynamic model of the cardiac sarcoplasmic/endoplasmic Ca2+ (SERCA) pump. *Biophys J* 2009;96:2029–2042.

Vance JE. Phospholipid synthesis in a membrane fraction associated with mitochondria. *J Biol Chem* 1990;265:7248–7256.

Vendelin M, Béraud N, Guerrero K, Andrienko T, Kuznetsov AV, Olivares J, Kay L, Saks VA. Mitochondrial regular arrangement in lmuscle cells: a "cristal-like" pattern. *Am J Physiol Cell Physiol* 2005;288:757–767.

Ventura-Clapier R, Garnier A, Veksler V. Transcriptional control of mitochondrial biogenesis: the central role of PGC-1α. *Cardiovasc Res* 2008;79:208–217.

Verde I, Vandecasteele G, Lezoualc'h F, Fischmeister R. Characterization of the cyclic nucleotide phosphodiesterase subtypes involved in the regulation of the L-type Ca2+ current in rat ventricular myocytes. *Br J Pharmacol* 1999;127:65–74.

Verkhratsky A, Toescu EC. Endoplasmic reticulum Ca2+ homeostasis and neuronal death. *J Cell Mol Med* 2003;7:351–361.

Verkhratsky A. Physiology and pathophysiology of the calcium store in the endoplasmic reticulum of neurons. *Physiol Rev* 2005;85:201–279.

Wang X, Su B, Lee HG, Li X, Perry G, Smith MA, Zhu X. Impaired balance of mitochondrial fission and fusion in Alzheimer's disease. *J Neurosci* 2009;29:9090–9103.

Wang YP, Fuchs F. Osmotic compression of skinned cardiac and skeletal muscle bundles: effects on force generation, Ca2+ sensitivity and Ca2+ binding. *J Mol Cell Cardiol* 1995;27:1235–1244.

Werth JL, Thayer SA. Mitochondria buffer physiological calcium loads in cultured rat dorsal root ganglion neurons. *J Neurosci* 1994;14:348–356.

Wilding JR, Joubert F, de Araujo C, Fortin D, Novotova M, Veksler V, Ventura-Clapier R. Altered energy transfer from mitochondria to sarcoplasmic reticulum after cytoarchidectural perturbations in mice hearts. *J Physiol* 2006;575:191–200.

Williamson TL, Cleveland DW. Slowing of axonal transport is a very early event in the toxicity of ALS-linked SOD1 mutants to motor neurons. *Nat Neurosci* 1999;2:50–56.

Wilson MG, Towner JW, Coffin GS, Ebbin AJ, Siris E, Brager P. Genetic and clinical studies in 13 patients with the Wolf-Hirschhorn syndrome [del(4p)]. *Hum Genet* 1981;59:297–307.

Wolf C, Mofrad MR. On the octagonal structure of the nuclear pore complex: insights from coarse-grained models. *Biophys J* 2008;95:2073–2085.

Wozniak MA, Chen CS. Mechanotransduction in development: a growing role for contractility. *Nat Rev Mol Cell Biol* 2009;10:34–43.

Xie LH, Takano M, Noma A. The inhibitory effect of propranolol on ATP-sensitive potassium channels in neonatal rat heart. ***Br J Pharmacol*** 1998;123:599–604.

Xu L, Tripathy A, Pasek DA, Meissner G. Ruthenium red modifies the cardiac and skeletal muscle Ca(2+) release channels (ryanodine receptors) by multiple mechanisms. *J Biol Chem* 1999;274:32680–32691.

Yagi N, Okuyama H, Toyota H, Araki J, Shimizu J, Iribe G, Nakamura K, Mohri S, Tsujioka K, Suga H, Kajiya F. Sarcomere-length dependence of lattice volume and radial mass transfer of myosin cross-bridges in rat papillary muscle. *Pflugers Arch* 2004;448:153–160.

Yamashita M, Sugioka M, Ogawa Y. Voltage- and Ca2+-activated potassium channels in Ca2+ store control Ca2+ release. *FEBS J* 2006;273:3585–3597.

Yi M, Weaver D, Hajnoczky G. Control of mitochondrial motility and distribution by the calcium signal. *J Cell Biol* 2004;167:661–672.

Zhang B, Tu P, Abtahian F, Trojanowski JQ, Lee VM. Neurofilaments and orthograde transport are reduced in ventral root axons of transgenic mice that express human SOD1 with a G93A mutation. *J Cell Biol* 1997;139:1307–1315.

Zhou M, Tanaka O, Sekiguchi M, He HJ, Yasuoka Y, Itoh H, Kawahara K, Abe H. ATP-sensitive K+-channel subunits on the mitochondria and endoplasmic reticulum of rat cardiomyocytes. *J Histochem Cytochem* 2005;53:1491–1500

Zlatanova J, Leuba SH. Stretching and imaging single DNA molecules and chromatin. *J Muscle Res Cell Motil* 2002;23:377–395.

Zollino M, Di Stefano C, Zampino G, Mastroiacovo P, Wright TJ, Sorge G, Selicorni A, Tenconi R, Zappala A, Battaglia A, Di Rocco M, Palka G, Pallotta R, Altherr MR, Neri G. Genotype-phenotype correlations and clinical diagnostic criteria in Wolf-Hirschhorn syndrome. *Am J Med Genet* 2000;94:254–261.

Zollino M, Lecce R, Fischetto R, Murdolo M, Faravelli F, Selicorni A, Butte C, Memo L, Capovilla G, Neri G. Mapping the Wolf-Hirschhorn syndrome phenotype outside the currently accepted WHS critical region and defining a new critical region, WHSCR-2. *Am J Hum Genet* 2003;72:590–597.

SUMMARY IN ESTONIAN

Katioonide voolud mitokondrites ja endoplasmaatilises retiikulumis: uued rollid raku füsioloogias

Mitokondrid on tuntud kui raku jõujaamad tootes enamiku rakule vajaminevast ATPst. Endoplasmaatilise retiikulumi põhifunktsiooniks on rakusisete Ca^{2+} voogude kontrollimine. Ehkki mitokondrid ja endoplasmaatiline retiikulum on eraldiseisvad organellid, on nende funktsioneerimine tihedalt üksteisega seotud ja tihti ka sarnaselt reguleeritud. Üheskoos mõjutavad nad mitmeid rakusiseseid protsesse nagu Ca^{2+} liikumist ja tasakaalu ning erinevaid signaalradasid ja rakusurma-mehhanisme.

Mitokondrite ja endoplasmaatilise retiikulumi funktsiooneerimisel mängivad olulist rolli rakusiseste katioonide, peamiselt kaaliumi ja kaltsiumi voolud. Mitokondri maatriksis olev kaalium kontrollib mitokondri mahtu, mis on oluline nii organelli terviklikkuse säilitamise kui ka funtsioneerimise seisukohalt. See on seotud nii mitokondrite energia tootmise kui ka programmeeritud rakusurma kaskaadi käivitamisega. Lisaks võivad muutused mitokondri mahus olla seotud ka muude, senini vähe uuritud protsessidega. Näiteks võib mitokondrite läbimõõdu suurenemine takistada aksonaalset transporti. Aksonaalse transpordi häired on seotud mitmete progresseeruvate neurodegeneratiivsete haigustega nagu Alzheimeri ja Huntingoni tõbi. Teisalt võivad paisunud mitokondrid südamelihasrakkudes mehhaaniliselt mõjutada ka naabruses olevaid rakustruktuure – näiteks müofilamente ja tuuma, mõjutades ühtlasi nende funktsiooni. See-eest lisaks varemmainitule mõjutab kaltsiumi kontsentratsioon mitokondri maatriksis ATP tootmist aktiveerides dehüdrogenaase Krebsi tsüklis ning võib põhjustada kaltsiumi ülekoormuse, mis omakorda võib viia rakusurma-mehhanismide käivitumiseni

Kaalium näib kontrollivat ka endoplasmaatilse retiikulumi funktsiooni. Endoplasmaatilise retiikulumi Ca^{2+} ülesvõtuga ei kaasne elektrokeemilise potensiaali teket endoplasmaatilise retiikulumi membraanil. See tähendab, et Ca^{2+} ülesvõttu tasakaalustab nn "vastasioonide" *(counter-ions)* (Na^+, K^+, Cl^-) liikumine läbi endoplasmaatilise retiikulumi membraani. Praeguse seisuga on neid ioone ning vastavaid ioonkanaleid endoplasmaatilise retiikulumi membraanis väga vähe uuritud.

Oluline on märkida, et endoplasmaatilise retiikulumi Ca^{2+} tase sõltub lisaks endoplasmaatilise retiikulumi Ca^{2+} ülesvõtule ka Ca^{2+} lekkimisest puhkeperioodil. See leke võib toimuda rüanodiini retseptorite kaudu või ka läbi SERCA. Arvatakse, et endoplasmaatilise retiikulumi Ca^{2+} leke võib sõltuda ka raku energeetilisest seisust. Lisaks võib suurenenud Ca^{2+} leke olla seotud südamepuudulikkuse kujunemisega...

Lähtuvalt eelnevast, oli töö eesmärgiks:

1) Hinnata, kuivõrd põhjustavad muutused katioonide voos läbi mitokondri sisemembraani mitokondrite paisumist närvirakkudes ning häirivad organellide transporti närvijätketes.
2) Uurida, kas mitokondrite mahu muutused südamelihasrakkudes võivad mehhaaniliselt mõjutada teisi rakusiseseid struktuure.
3) Uurida kaaliumi voolude olemust ja rolli endoplasmaatilise retiikulumi kaltsiumi ülesvõtus.
4) Selgitada, milline on peamine Ca^{2+} lekke mehhanism südamelihasrakkudes ja millised tegurid võivad seda kaltsiumi leket mõjutada.

Antud töö tulemustest võime järeldada et,

1) Paisunud mitokondrid võivad halvendada aksonaalset transporti neuronites takistades füüsiliselt nii mitokondrite kui lüsosoomide liikumist. See omakorda võib häirida närvirakkude funktsioneerimist ja olla seotud ka neurodegeneratiivsete haiguste tekkemehhanismidega.
2) Paisunud mitokondrid genereerivad rakusiseseid jõude, mis võivad südamelihasrakkudes põhjustada nii müofilamentide kui tuuma kompressiooni. Selle kaudu võivad nad mõjutada nii kontraktiilsust kui ka tuuma funktsioneerimist.
3) Kaaliumi voolud läbi endoplasmaatilise retiikulumi KHE ja SK_{Ca} kanalite mängivad olulist rolli endoplasmaatilise retiikulumi Ca^{2+} ülesvõtus nii neuronites kui kardiomüotsüütides.
4) SERCA mängib olulist rolli Ca^{2+} lekkes endoplasmaatilise retiikulumi luumenist ning see leke sõltub südamelihase energeetilisest seisundist.

ACKNOWLEDGEMENTS

This study was carried out at the Department of Pharmacology, University of Tartu, Estonia and Faculty of Pharmacy, U-769 INSERM, Université Paris-Sud, Châtenay-Malabry, France. The study was financially supported by Estonian Science Foundation, The European Regional Development Fund, European Community, ARCHIMEDES Foundation, Institut National de la Santé et de la Recherche Médicale.

I would like to express my deepest gratitude to everyone, who has stayed with me and guided me during my doctoral studies.

In particular, sincere thanks to:
- My supervisors professor Vladimir Veksler and professor Allen Kaasik for their support, encouragement and patience.
- Researcher, Frederic Joubert, for guidance and support.
- Entire staff of the Departament of Pharmacology at the University of Tartu for their help and friendly atmosphere.
- Entire staff of the U-769 INSERM "Signalisation et Physiopathologie Cardiaque" at the Université Paris-Sud for their help and good company.
- My friends for their support and understanding.
- My fellow students while doctoral studies and best friends, Anu and Madis, whithout who I would not have made this.
- My family for their love, support and giving me the possibilities for educating myself.

PUBLICATIONS

CURRICULUM VITAE

Malle Kuum

Date and place of birth:	November 5, 1982, Tartu, Estonia
Citizenship:	Estonian
Address:	Mõisavahe 46–31, Tartu 50708, Estonia
Telefon:	+372 737 4367
e-mail:	malle_k@ut.ee

Education

2005– …	University of Tartu, Faculty of Medicine, Doctoral program of Medicine
2000–2005	University of Tartu, Pharmacy
1989–2000	Tartu Mart Reiniku Gymnasium

Employment history

2009– …	University of Tartu, Department of Pharmacology, specialist
2008–2009	Mõisavahe Pharmacy, pharmacist
2005	Mõisavahe Pharmacy, pharmacist
2003	Mai Pharmacy, technician

Special courses

2010	Palmse Mois Summer School 2010, Palmse, Estonia
2007	Laboratory Animal Science C – Category Competence Course, Tartu, Estonia
2007	Mitocourse 2007, Tartu, Estonia

Professional organizations

Estonian Society of Pharmacology

Scientific work

Ca^{2+} circulation and regulatory mechanisms of Ca^{2+} fluxes of sarco(endo)-plasmic reticulum.
Novel roles of mitochondria in functioning of the neuronal system and the heart.

CURRICULUM VITAE

Malle Kuum

Sünniaeg ja koht:	05.11.1982, Tartu
Kodakondsus:	Eesti
Aadress:	Mõisavahe 46–31, Tartu 50708, Eesti
Telefon:	+372 737 4367
e-mail:	malle_k@ut.ee

Haridus

2005– …	Tartu Ülikool, Arstiteaduskond, arstiteaduse doktoriõpe, doktorant
2000–2005	Tartu Ülikool, proviisoriõpe
1989–2000	Tartu Mart Reiniku Gümnaasium

Teenistuskäik

2009– …	Tartu Ülikool, Farmakoloogia instituut, spetsialist
2008–2009	Mõisavahe apteek, proviisor
2005	Mõisavahe apteek, proviisor
2003	Mai apteek, tehnik

Erialane enesetäiendus

2010	Palmse Mois Summer School 2010, Palmse, Eesti
2007	Katseloomateaduse C– kategooria kursus, Tartu, Eesti
2007	Mitocourse 2007, Tartu, Eesti

Erialaorganisatsioonid

Eesti Farmakoloogia Selts

Peamised uurimisvaldkonnad

Kaltsiumi ringlus ja selle regulatsiooni mehhanismid sarko(endo)plasmaatilises retiikulumis.
Mitokondrite uued rollid närvisüsteemi ja südame funktsioonis.

DISSERTATIONES MEDICINAE UNIVERSITATIS TARTUENSIS

1. **Heidi-Ingrid Maaroos.** The natural course of gastric ulcer in connection with chronic gastritis and *Helicobacter pylori*. Tartu, 1991.
2. **Mihkel Zilmer.** Na-pump in normal and tumorous brain tissues: Structural, functional and tumorigenesis aspects. Tartu, 1991.
3. **Eero Vasar.** Role of cholecystokinin receptors in the regulation of behaviour and in the action of haloperidol and diazepam. Tartu, 1992.
4. **Tiina Talvik.** Hypoxic-ischaemic brain damage in neonates (clinical, biochemical and brain computed tomographical investigation). Tartu, 1992.
5. **Ants Peetsalu.** Vagotomy in duodenal ulcer disease: A study of gastric acidity, serum pepsinogen I, gastric mucosal histology and *Helicobacter pylori*. Tartu, 1992.
6. **Marika Mikelsaar.** Evaluation of the gastrointestinal microbial ecosystem in health and disease. Tartu, 1992.
7. **Hele Everaus.** Immuno-hormonal interactions in chronic lymphocytic leukaemia and multiple myeloma. Tartu, 1993.
8. **Ruth Mikelsaar.** Etiological factors of diseases in genetically consulted children and newborn screening: dissertation for the commencement of the degree of doctor of medical sciences. Tartu, 1993.
9. **Agu Tamm.** On metabolic action of intestinal microflora: clinical aspects. Tartu, 1993.
10. **Katrin Gross.** Multiple sclerosis in South-Estonia (epidemiological and computed tomographical investigations). Tartu, 1993.
11. **Oivi Uibo.** Childhood coeliac disease in Estonia: occurrence, screening, diagnosis and clinical characterization. Tartu, 1994.
12. **Viiu Tuulik.** The functional disorders of central nervous system of chemistry workers. Tartu, 1994.
13. **Margus Viigimaa.** Primary haemostasis, antiaggregative and anticoagulant treatment of acute myocardial infarction. Tartu, 1994.
14. **Rein Kolk.** Atrial versus ventricular pacing in patients with sick sinus syndrome. Tartu, 1994.
15. **Toomas Podar.** Incidence of childhood onset type 1 diabetes mellitus in Estonia. Tartu, 1994.
16. **Kiira Subi.** The laboratory surveillance of the acute respiratory viral infections in Estonia. Tartu, 1995.
17. **Irja Lutsar.** Infections of the central nervous system in children (epidemiologic, diagnostic and therapeutic aspects, long term outcome). Tartu, 1995.
18. **Aavo Lang.** The role of dopamine, 5-hydroxytryptamine, sigma and NMDA receptors in the action of antipsychotic drugs. Tartu, 1995.
19. **Andrus Arak.** Factors influencing the survival of patients after radical surgery for gastric cancer. Tartu, 1996.
20. **Tõnis Karki.** Quantitative composition of the human lactoflora and method for its examination. Tartu, 1996.

21. **Reet Mändar.** Vaginal microflora during pregnancy and its transmission to newborn. Tartu, 1996.
22. **Triin Remmel.** Primary biliary cirrhosis in Estonia: epidemiology, clinical characterization and prognostication of the course of the disease. Tartu, 1996.
23. **Toomas Kivastik.** Mechanisms of drug addiction: focus on positive reinforcing properties of morphine. Tartu, 1996.
24. **Paavo Pokk.** Stress due to sleep deprivation: focus on $GABA_A$ receptor-chloride ionophore complex. Tartu, 1996.
25. **Kristina Allikmets.** Renin system activity in essential hypertension. Associations with atherothrombogenic cardiovascular risk factors and with the efficacy of calcium antagonist treatment. Tartu, 1996.
26. **Triin Parik.** Oxidative stress in essential hypertension: Associations with metabolic disturbances and the effects of calcium antagonist treatment. Tartu, 1996.
27. **Svetlana Päi.** Factors promoting heterogeneity of the course of rheumatoid arthritis. Tartu, 1997.
28. **Maarike Sallo.** Studies on habitual physical activity and aerobic fitness in 4 to 10 years old children. Tartu, 1997.
29. **Paul Naaber.** *Clostridium difficile* infection and intestinal microbial ecology. Tartu, 1997.
30. **Rein Pähkla.** Studies in pinoline pharmacology. Tartu, 1997.
31. **Andrus Juhan Voitk.** Outpatient laparoscopic cholecystectomy. Tartu, 1997.
32. **Joel Starkopf.** Oxidative stress and ischaemia-reperfusion of the heart. Tartu, 1997.
33. **Janika Kõrv.** Incidence, case-fatality and outcome of stroke. Tartu, 1998.
34. **Ülla Linnamägi.** Changes in local cerebral blood flow and lipid peroxidation following lead exposure in experiment. Tartu, 1998.
35. **Ave Minajeva.** Sarcoplasmic reticulum function: comparison of atrial and ventricular myocardium. Tartu, 1998.
36. **Oleg Milenin.** Reconstruction of cervical part of esophagus by revascularised ileal autografts in dogs. A new complex multistage method. Tartu, 1998.
37. **Sergei Pakriev.** Prevalence of depression, harmful use of alcohol and alcohol dependence among rural population in Udmurtia. Tartu, 1998.
38. **Allen Kaasik.** Thyroid hormone control over β-adrenergic signalling system in rat atria. Tartu, 1998.
39. **Vallo Matto.** Pharmacological studies on anxiogenic and antiaggressive properties of antidepressants. Tartu, 1998.
40. **Maire Vasar.** Allergic diseases and bronchial hyperreactivity in Estonian children in relation to environmental influences. Tartu, 1998.
41. **Kaja Julge.** Humoral immune responses to allergens in early childhood. Tartu, 1998.
42. **Heli Grünberg.** The cardiovascular risk of Estonian schoolchildren. A cross-sectional study of 9-, 12- and 15-year-old children. Tartu, 1998.

43. **Epp Sepp.** Formation of intestinal microbial ecosystem in children. Tartu, 1998.
44. **Mai Ots.** Characteristics of the progression of human and experimental glomerulopathies. Tartu, 1998.
45. **Tiina Ristimäe.** Heart rate variability in patients with coronary artery disease. Tartu, 1998.
46. **Leho Kõiv.** Reaction of the sympatho-adrenal and hypothalamo-pituitary-adrenocortical system in the acute stage of head injury. Tartu, 1998.
47. **Bela Adojaan.** Immune and genetic factors of childhood onset IDDM in Estonia. An epidemiological study. Tartu, 1999.
48. **Jakov Shlik.** Psychophysiological effects of cholecystokinin in humans. Tartu, 1999.
49. **Kai Kisand.** Autoantibodies against dehydrogenases of α-ketoacids. Tartu, 1999.
50. **Toomas Marandi.** Drug treatment of depression in Estonia. Tartu, 1999.
51. **Ants Kask.** Behavioural studies on neuropeptide Y. Tartu, 1999.
52. **Ello-Rahel Karelson.** Modulation of adenylate cyclase activity in the rat hippocampus by neuropeptide galanin and its chimeric analogs. Tartu, 1999.
53. **Tanel Laisaar.** Treatment of pleural empyema — special reference to intrapleural therapy with streptokinase and surgical treatment modalities. Tartu, 1999.
54. **Eve Pihl.** Cardiovascular risk factors in middle-aged former athletes. Tartu, 1999.
55. **Katrin Õunap.** Phenylketonuria in Estonia: incidence, newborn screening, diagnosis, clinical characterization and genotype/phenotype correlation. Tartu, 1999.
56. **Siiri Kõljalg.** *Acinetobacter* – an important nosocomial pathogen. Tartu, 1999.
57. **Helle Karro.** Reproductive health and pregnancy outcome in Estonia: association with different factors. Tartu, 1999.
58. **Heili Varendi.** Behavioral effects observed in human newborns during exposure to naturally occurring odors. Tartu, 1999.
59. **Anneli Beilmann.** Epidemiology of epilepsy in children and adolescents in Estonia. Prevalence, incidence, and clinical characteristics. Tartu, 1999.
60. **Vallo Volke.** Pharmacological and biochemical studies on nitric oxide in the regulation of behaviour. Tartu, 1999.
61. **Pilvi Ilves.** Hypoxic-ischaemic encephalopathy in asphyxiated term infants. A prospective clinical, biochemical, ultrasonographical study. Tartu, 1999.
62. **Anti Kalda.** Oxygen-glucose deprivation-induced neuronal death and its pharmacological prevention in cerebellar granule cells. Tartu, 1999.
63. **Eve-Irene Lepist.** Oral peptide prodrugs – studies on stability and absorption. Tartu, 2000.
64. **Jana Kivastik.** Lung function in Estonian schoolchildren: relationship with anthropometric indices and respiratory symptomas, reference values for dynamic spirometry. Tartu, 2000.

65. **Karin Kull.** Inflammatory bowel disease: an immunogenetic study. Tartu, 2000.
66. **Kaire Innos.** Epidemiological resources in Estonia: data sources, their quality and feasibility of cohort studies. Tartu, 2000.
67. **Tamara Vorobjova.** Immune response to *Helicobacter pylori* and its association with dynamics of chronic gastritis and epithelial cell turnover in antrum and corpus. Tartu, 2001.
68. **Ruth Kalda.** Structure and outcome of family practice quality in the changing health care system of Estonia. Tartu, 2001.
69. **Annika Krüüner.** *Mycobacterium tuberculosis* – spread and drug resistance in Estonia. Tartu, 2001.
70. **Marlit Veldi.** Obstructive Sleep Apnoea: Computerized Endopharyngeal Myotonometry of the Soft Palate and Lingual Musculature. Tartu, 2001.
71. **Anneli Uusküla.** Epidemiology of sexually transmitted diseases in Estonia in 1990–2000. Tartu, 2001.
72. **Ade Kallas.** Characterization of antibodies to coagulation factor VIII. Tartu, 2002.
73. **Heidi Annuk.** Selection of medicinal plants and intestinal lactobacilli as antimicrobil components for functional foods. Tartu, 2002.
74. **Aet Lukmann**. Early rehabilitation of patients with ischaemic heart disease after surgical revascularization of the myocardium: assessment of health-related quality of life, cardiopulmonary reserve and oxidative stress. A clinical study. Tartu, 2002.
75. **Maigi Eisen.** Pathogenesis of Contact Dermatitis: participation of Oxidative Stress. A clinical – biochemical study. Tartu, 2002.
76. **Piret Hussar.** Histology of the post-traumatic bone repair in rats. Elaboration and use of a new standardized experimental model – bicortical perforation of tibia compared to internal fracture and resection osteotomy. Tartu, 2002.
77. **Tõnu Rätsep.** Aneurysmal subarachnoid haemorrhage: Noninvasive monitoring of cerebral haemodynamics. Tartu, 2002.
78. **Marju Herodes.** Quality of life of people with epilepsy in Estonia. Tartu, 2003.
79. **Katre Maasalu.** Changes in bone quality due to age and genetic disorders and their clinical expressions in Estonia. Tartu, 2003.
80. **Toomas Sillakivi.** Perforated peptic ulcer in Estonia: epidemiology, risk factors and relations with *Helicobacter pylori*. Tartu, 2003.
81. **Leena Puksa.** Late responses in motor nerve conduction studies. F and A waves in normal subjects and patients with neuropathies. Tartu, 2003.
82. **Krista Lõivukene**. *Helicobacter pylori* in gastric microbial ecology and its antimicrobial susceptibility pattern. Tartu, 2003.
83. **Helgi Kolk.** Dyspepsia and *Helicobacter pylori* infection: the diagnostic value of symptoms, treatment and follow-up of patients referred for upper gastrointestinal endoscopy by family physicians. Tartu, 2003.

84. **Helena Soomer.** Validation of identification and age estimation methods in forensic odontology. Tartu, 2003.
85. **Kersti Oselin.** Studies on the human MDR1, MRP1, and MRP2 ABC transporters: functional relevance of the genetic polymorphisms in the *MDR1* and *MRP1* gene. Tartu, 2003.
86. **Jaan Soplepmann.** Peptic ulcer haemorrhage in Estonia: epidemiology, prognostic factors, treatment and outcome. Tartu, 2003.
87. **Margot Peetsalu.** Long-term follow-up after vagotomy in duodenal ulcer disease: recurrent ulcer, changes in the function, morphology and *Helicobacter pylori* colonisation of the gastric mucosa. Tartu, 2003.
88. **Kersti Klaamas.** Humoral immune response to *Helicobacter pylori* a study of host-dependent and microbial factors. Tartu, 2003.
89. **Pille Taba.** Epidemiology of Parkinson's disease in Tartu, Estonia. Prevalence, incidence, clinical characteristics, and pharmacoepidemiology. Tartu, 2003.
90. **Alar Veraksitš**. Characterization of behavioural and biochemical phenotype of cholecystokinin-2 receptor deficient mice: changes in the function of the dopamine and endopioidergic system. Tartu, 2003.
91. **Ingrid Kalev.** CC-chemokine receptor 5 (CCR5) gene polymorphism in Estonians and in patients with Type I and Type II diabetes mellitus. Tartu, 2003.
92. **Lumme Kadaja.** Molecular approach to the regulation of mitochondrial function in oxidative muscle cells. Tartu, 2003.
93. **Aive Liigant**. Epidemiology of primary central nervous system tumours in Estonia from 1986 to 1996. Clinical characteristics, incidence, survival and prognostic factors. Tartu, 2004.
94. **Andres, Kulla.** Molecular characteristics of mesenchymal stroma in human astrocytic gliomas. Tartu, 2004.
95. **Mari Järvelaid.** Health damaging risk behaviours in adolescence. Tartu, 2004.
96. **Ülle Pechter.** Progression prevention strategies in chronic renal failure and hypertension. An experimental and clinical study. Tartu, 2004.
97. **Gunnar Tasa.** Polymorphic glutathione S-transferases – biology and role in modifying genetic susceptibility to senile cataract and primary open angle glaucoma. Tartu, 2004.
98. **Tuuli Käämbre.** Intracellular energetic unit: structural and functional aspects. Tartu, 2004.
99. **Vitali Vassiljev.** Influence of nitric oxide syntase inhibitors on the effects of ethanol after acute and chronic ethanol administration and withdrawal. Tartu, 2004.
100. **Aune Rehema.** Assessment of nonhaem ferrous iron and glutathione redox ratio as markers of pathogeneticity of oxidative stress in different clinical groups. Tartu, 2004.
101. **Evelin Seppet.** Interaction of mitochondria and ATPases in oxidative muscle cells in normal and pathological conditions. Tartu, 2004.

102. **Eduard Maron.** Serotonin function in panic disorder: from clinical experiments to brain imaging and genetics. Tartu, 2004.
103. **Marje Oona.** *Helicobacter pylori* infection in children: epidemiological and therapeutic aspects. Tartu, 2004.
104. **Kersti Kokk.** Regulation of active and passive molecular transport in the testis. Tartu, 2005.
105. **Vladimir Järv.** Cross-sectional imaging for pretreatment evaluation and follow-up of pelvic malignant tumours. Tartu, 2005.
106. **Andre Õun.** Epidemiology of adult epilepsy in Tartu, Estonia. Incidence, prevalence and medical treatment. Tartu, 2005.
107. **Piibe Muda.** Homocysteine and hypertension: associations between homocysteine and essential hypertension in treated and untreated hypertensive patients with and without coronary artery disease. Tartu, 2005.
108. **Külli Kingo.** The interleukin-10 family cytokines gene polymorphisms in plaque psoriasis. Tartu, 2005.
109. **Mati Merila.** Anatomy and clinical relevance of the glenohumeral joint capsule and ligaments. Tartu, 2005.
110. **Epp Songisepp**. Evaluation of technological and functional properties of the new probiotic *Lactobacillus fermentum* ME-3. Tartu, 2005.
111. **Tiia Ainla.** Acute myocardial infarction in Estonia: clinical characteristics, management and outcome. Tartu, 2005.
112. **Andres Sell.** Determining the minimum local anaesthetic requirements for hip replacement surgery under spinal anaesthesia – a study employing a spinal catheter. Tartu, 2005.
113. **Tiia Tamme.** Epidemiology of odontogenic tumours in Estonia. Pathogenesis and clinical behaviour of ameloblastoma. Tartu, 2005.
114. **Triine Annus**. Allergy in Estonian schoolchildren: time trends and characteristics. Tartu, 2005.
115. **Tiia Voor.** Microorganisms in infancy and development of allergy: comparison of Estonian and Swedish children. Tartu, 2005.
116. **Priit Kasenõmm.** Indicators for tonsillectomy in adults with recurrent tonsillitis – clinical, microbiological and pathomorphological investigations. Tartu, 2005.
117. **Eva Zusinaite.** Hepatitis C virus: genotype identification and interactions between viral proteases. Tartu, 2005.
118. **Piret Kõll.** Oral lactoflora in chronic periodontitis and periodontal health. Tartu, 2006.
119. **Tiina Stelmach.** Epidemiology of cerebral palsy and unfavourable neurodevelopmental outcome in child population of Tartu city and county, Estonia Prevalence, clinical features and risk factors. Tartu, 2006.
120. **Katrin Pudersell.** Tropane alkaloid production and riboflavine excretion in the field and tissue cultures of henbane (*Hyoscyamus niger* L.). Tartu, 2006.
121. **Külli Jaako.** Studies on the role of neurogenesis in brain plasticity. Tartu, 2006.

35

122. **Aare Märtson.** Lower limb lengthening: experimental studies of bone regeneration and long-term clinical results. Tartu, 2006.
123. **Heli Tähepõld.** Patient consultation in family medicine. Tartu, 2006.
124. **Stanislav Liskmann.** Peri-implant disease: pathogenesis, diagnosis and treatment in view of both inflammation and oxidative stress profiling. Tartu, 2006.
125. **Ruth Rudissaar.** Neuropharmacology of atypical antipsychotics and an animal model of psychosis. Tartu, 2006.
126. **Helena Andreson.** Diversity of *Helicobacter pylori* genotypes in Estonian patients with chronic inflammatory gastric diseases. Tartu, 2006.
127. **Katrin Pruus.** Mechanism of action of antidepressants: aspects of serotoninergic system and its interaction with glutamate. Tartu, 2006.
128. **Priit Põder.** Clinical and experimental investigation: relationship of ischaemia/reperfusion injury with oxidative stress in abdominal aortic aneurysm repair and in extracranial brain artery endarterectomy and possibilities of protection against ischaemia using a glutathione analogue in a rat model of global brain ischaemia. Tartu, 2006.
129. **Marika Tammaru.** Patient-reported outcome measurement in rheumatoid arthritis. Tartu, 2006.
130. **Tiia Reimand.** Down syndrome in Estonia. Tartu, 2006.
131. **Diva Eensoo.** Risk-taking in traffic and Markers of Risk-Taking Behaviour in Schoolchildren and Car Drivers. Tartu, 2007.
132. **Riina Vibo.** The third stroke registry in Tartu, Estonia from 2001 to 2003: incidence, case-fatality, risk factors and long-term outcome. Tartu, 2007.
133. **Chris Pruunsild.** Juvenile idiopathic arthritis in children in Estonia. Tartu, 2007.
134. **Eve Õiglane-Šlik.** Angelman and Prader-Willi syndromes in Estonia. Tartu, 2007.
135. **Kadri Haller.** Antibodies to follicle stimulating hormone. Significance in female infertility. Tartu, 2007.
136. **Pille Ööpik.** Management of depression in family medicine. Tartu, 2007.
137. **Jaak Kals.** Endothelial function and arterial stiffness in patients with atherosclerosis and in healthy subjects. Tartu, 2007.
138. **Priit Kampus.** Impact of inflammation, oxidative stress and age on arterial stiffness and carotid artery intima-media thickness. Tartu, 2007.
139. **Margus Punab.** Male fertility and its risk factors in Estonia. Tartu, 2007.
140. **Alar Toom**. Heterotopic ossification after total hip arthroplasty: clinical and pathogenetic investigation. Tartu, 2007.
141. **Lea Pehme.** Epidemiology of tuberculosis in Estonia 1991–2003 with special regard to extrapulmonary tuberculosis and delay in diagnosis of pulmonary tuberculosis. Tartu, 2007.
142. **Juri Karjagin.** The pharmacokinetics of metronidazole and meropenem in septic shock. Tartu, 2007.
143. **Inga Talvik.** Inflicted traumatic brain injury shaken baby syndrome in Estonia – epidemiology and outcome. Tartu, 2007.

144. **Tarvo Rajasalu.** Autoimmune diabetes: an immunological study of type 1 diabetes in humans and in a model of experimental diabetes (in RIP-B7.1 mice). Tartu, 2007.
145. **Inga Karu.** Ischaemia-reperfusion injury of the heart during coronary surgery: a clinical study investigating the effect of hyperoxia. Tartu, 2007.
146. **Peeter Padrik.** Renal cell carcinoma: Changes in natural history and treatment of metastatic disease. Tartu, 2007.
147. **Neve Vendt.** Iron deficiency and iron deficiency anaemia in infants aged 9 to 12 months in Estonia. Tartu, 2008.
148. **Lenne-Triin Heidmets.** The effects of neurotoxins on brain plasticity: focus on neural Cell Adhesion Molecule. Tartu, 2008.
149. **Paul Korrovits.** Asymptomatic inflammatory prostatitis: prevalence, etiological factors, diagnostic tools. Tartu, 2008.
150. **Annika Reintam.** Gastrointestinal failure in intensive care patients. Tartu, 2008.
151. **Kristiina Roots.** Cationic regulation of Na-pump in the normal, Alzheimer's and CCK_2 receptor-deficient brain. Tartu, 2008.
152. **Helen Puusepp.** The genetic causes of mental retardation in Estonia: fragile X syndrome and creatine transporter defect. Tartu, 2009.
153. **Kristiina Rull.** Human chorionic gonadotropin beta genes and recurrent miscarriage: expression and variation study. Tartu, 2009.
154. **Margus Eimre.** Organization of energy transfer and feedback regulation in oxidative muscle cells. Tartu, 2009.
155. **Maire Link.** Transcription factors FoxP3 and AIRE: autoantibody associations. Tartu, 2009.
156. **Kai Haldre.** Sexual health and behaviour of young women in Estonia. Tartu, 2009.
157. **Kaur Liivak.** Classical form of congenital adrenal hyperplasia due to 21-hydroxylase deficiency in Estonia: incidence, genotype and phenotype with special attention to short-term growth and 24-hour blood pressure. Tartu, 2009.
158. **Kersti Ehrlich.** Antioxidative glutathione analogues (UPF peptides) – molecular design, structure-activity relationships and testing the protective properties. Tartu, 2009.
159. **Anneli Rätsep.** Type 2 diabetes care in family medicine. Tartu, 2009.
160. **Silver Türk.** Etiopathogenetic aspects of chronic prostatitis: role of mycoplasmas, coryneform bacteria and oxidative stress. Tartu, 2009.
161. **Kaire Heilman.** Risk markers for cardiovascular disease and low bone mineral density in children with type 1 diabetes. Tartu, 2009.
162. **Kristi Rüütel.** HIV-epidemic in Estonia: injecting drug use and quality of life of people living with HIV. Tartu, 2009.
163. **Triin Eller.** Immune markers in major depression and in antidepressive treatment. Tartu, 2009.

164. **Siim Suutre.** The role of TGF-β isoforms and osteoprogenitor cells in the pathogenesis of heterotopic ossification. An experimental and clinical study of hip arthroplasty. Tartu, 2010.
165. **Kai Kliiman.** Highly drug-resistant tuberculosis in Estonia: Risk factors and predictors of poor treatment outcome. Tartu, 2010.
166. **Inga Villa.** Cardiovascular health-related nutrition, physical activity and fitness in Estonia. Tartu, 2010.
167. **Tõnis Org.** Molecular function of the first PHD finger domain of Autoimmune Regulator protein. Tartu, 2010.
168. **Tuuli Metsvaht.** Optimal antibacterial therapy of neonates at risk of early onset sepsis. Tartu, 2010.
169. **Jaanus Kahu.** Kidney transplantation: Studies on donor risk factors and mycophenolate mofetil. Tartu, 2010.
170. **Koit Reimand.** Autoimmunity in reproductive failure: A study on associated autoantibodies and autoantigens. Tartu, 2010.
171. **Mart Kull.** Impact of vitamin D and hypolactasia on bone mineral density: a population based study in Estonia. Tartu, 2010.
172. **Rael Laugesaar.** Stroke in children – epidemiology and risk factors. Tartu, 2010.
173. **Mark Braschinsky.** Epidemiology and quality of life issues of hereditary spastic paraplegia in Estonia and implemention of genetic analysis in everyday neurologic practice. Tartu, 2010.
174. **Kadri Suija.** Major depression in family medicine: associated factors, recurrence and possible intervention. Tartu, 2010.
175. **Jarno Habicht.** Health care utilisation in Estonia: socioeconomic determinants and financial burden of out-of-pocket payments. Tartu, 2010.
176. **Kristi Abram.** The prevalence and risk factors of rosacea. Subjective disease perception of rosacea patients. Tartu, 2010.